

# Optimization of anti-CD19 CAR T cell production for treatment of patients with chronic lymphocytic leukemia

Christina Amaty,<sup>1</sup> Katherine A. Weissler,<sup>1</sup> Vicki Fellowes,<sup>2</sup> Norris Lam,<sup>1</sup> Lauren C. Cutmore,<sup>1</sup> Danielle A. Natrakul,<sup>1</sup> Steven L. Highfill,<sup>2</sup> and James N. Kochenderfer<sup>1</sup>

<sup>1</sup>National Institutes of Health, National Cancer Institute, Center for Cancer Research, Surgery Branch Bethesda, Bethesda, MD, USA; <sup>2</sup>Center for Cellular Engineering, Department of Transfusion Medicine, National Institutes of Health, Bethesda, MD, USA

**T cells expressing anti-CD19 chimeric antigen receptors (CARs) have activity against chronic lymphocytic leukemia (CLL), but complete response rates range from 18% to 29%, so improvement is needed. Peripheral blood mononuclear cells (PBMCs) of CLL patients often contain high levels of CLL cells that can interfere with CAR T cell production, and T cells from CLL patients are prone to exhaustion and other functional defects. We previously developed an anti-CD19 CAR designated Hu19-CD828Z. Hu19-CD828Z has a binding domain derived from a fully human antibody and a CD28 costimulatory domain. We aimed to develop an optimized process for producing Hu19-CD828Z-expressing T cells (Hu19-CAR T) from PBMC of CLL patients. We determined that supplementing Hu19-CAR-T cultures with interleukin (IL)-7 + IL-15 had advantages over using IL-2, including greater accumulation of Hu19-CAR T cells during *in vitro* proliferation assays. We determined that positive selection with anti-CD4 and anti-CD8 magnetic beads was the optimal method of T cell purification because this method resulted in high T cell purity. We determined that anti-CD3/CD28 paramagnetic beads were the optimal T cell activation reagent. Finally, we developed a current good manufacturing practices-compliant clinical-scale protocol for producing Hu19-CAR T from PBMC of CLL patients. These Hu19-CAR T exhibited a full range of *in vitro* functions and eliminated leukemia from mice.**

## INTRODUCTION

Chronic lymphocytic leukemia (CLL) is one of the most common hematological malignancies with an estimated incidence of 18,740 in the United States for 2023.<sup>1</sup> CLL is a clonal proliferation of CD19<sup>+</sup>CD5<sup>+</sup> B cells in bone marrow, blood, lymph nodes, and spleen.<sup>2,3</sup> Current treatment options for CLL, including chemotherapy and small molecule drugs such as ibrutinib, can be effective, but these treatments are not curative.<sup>2-4</sup> Monoclonal antibodies such as the anti-CD20 antibody rituximab (Rtx) are also non-curative treatments for CLL.<sup>5,6</sup> Allogeneic hematopoietic stem cell transplantation (alloHSCT) can cure CLL, but alloHSCT has a non-relapse mortality rate of 15%–25%, and chronic graft-versus-host disease is a significant problem.<sup>7,8</sup> Improved treatments for CLL are needed.

Chimeric antigen receptors (CARs) are artificial fusion proteins that contain an antigen-recognition domain that is usually a single chain variable fragment (scFv), a hinge domain, a transmembrane domain, and intracellular signaling domains.<sup>9-11</sup> T cells expressing CARs targeting CD19 are effective therapies for B-cell lymphoma and acute lymphoblastic leukemia.<sup>12-18</sup> CD19 is expressed on the surface of CLL cells,<sup>19</sup> so anti-CD19 CAR T cells are a rational therapy for CLL. Early anti-CD19 CAR clinical trials demonstrated activity against CLL.<sup>20-23</sup> Later single-center clinical trials evaluating anti-CD19 CAR T cells against CLL had complete remission (CR) rates of 21%–29% and median progression-free survivals (PFSs) of 1–8.5 months.<sup>24-26</sup> In a multicenter clinical trial of the anti-CD19 CAR T cell product lisocabtagene maraleucel, the 49 patients in the primary efficacy assessment subset had a CR rate of 18% and a PFS of 11.9 months.<sup>27</sup> All patients on the primary efficacy assessment subset of this study had experienced failure of venetoclax therapy and progressive CLL while on ibrutinib prior to study enrollment.<sup>27</sup> Overall, results from these clinical trials of anti-CD19 CARs for CLL demonstrated significant anti-leukemia activity; however, CR rates and PFSs are lower than the results obtained treating B-cell lymphoma with anti-CD19 CAR T cells,<sup>13,14,28</sup> so there is room for improvement in anti-CD19 CAR T cell therapy for CLL.

There are various factors that make CAR T cell therapy challenging in CLL patients. The blood of patients with CLL often contains a high percentage of leukemia cells, so methods of T cell purification are needed as an early step in clinical CAR T cell production.<sup>29</sup> Compared with T cells from healthy donors, T cells from CLL patients are more susceptible to exhaustion and have functional defects, possibly due to prolonged exposure to CLL cells.<sup>30,31</sup> Anti-CD19 CAR T cell products with effector or exhausted gene signatures have been associated with a limited ability to induce remission in CLL.<sup>32</sup>

Received 26 September 2023; accepted 12 February 2024;  
<https://doi.org/10.1016/j.omtm.2024.101212>.

**Correspondence:** James N. Kochenderfer, NIH, 10 Center Drive CRC Room 3-3330, Bethesda, MD 20892, USA.

**E-mail:** [kochendj@mail.nih.gov](mailto:kochendj@mail.nih.gov)



There have been two commonly used methods of T cell purification in CLL CAR clinical trials.<sup>24,25</sup> Paramagnetic beads coated with antibodies against CD3 and CD28 (Dynabeads™ [dyna]) have been used for both T cell purification and T cell activation.<sup>25</sup> Magnetic separation with the CliniMACS system has also been used.<sup>24</sup> In some trials, CD4<sup>+</sup> and CD8<sup>+</sup> T cell subsets were purified with the CliniMACS system, and these subsets were activated separately with dynas. The final CAR T cell product was then infused with an equal ratio of CD4<sup>+</sup> to CD8<sup>+</sup> T cells.<sup>24</sup> Different clinical trials have used different methods of T cell activation, but the most commonly used method has been dyna.<sup>23–25</sup> In prior anti-CD19 CAR clinical trials for CLL, either interleukin (IL)-2 or a combination of IL-7 and IL-15 (IL-7+IL-15) have been added to CAR T cell culture media.<sup>20,26,33</sup> Prior preclinical studies comparing CAR T cells cultured with IL-2 or IL-7+IL-15 have reported that IL-7+IL-15 increased T memory stem cells (Tscm) and enhanced anti-tumor efficacy.<sup>34,35</sup>

In this study, we evaluated different strategies for CAR T cell preparation to optimize production of anti-CD19 CAR T cells from peripheral blood mononuclear cells (PBMCs) of CLL patients. We utilized an anti-CD19 CAR called Hu19-CD828Z, which has a scFv derived from a human anti-CD19 antibody, hinge and transmembrane domains from CD8 $\alpha$ , a CD28 costimulatory domain, and a CD3 $\zeta$  T cell activation moiety.<sup>36</sup> T cells expressing Hu19-CD828Z have been shown to be effective against lymphoma and to have a low incidence of neurological toxicity in a previous clinical trial conducted by our group.<sup>17,37</sup> For this study, we examined different methods to purify T cells from CLL cells, different reagents to activate the T cells, and different cytokines added to the CAR T cell culture media. We developed an optimized protocol for producing autologous anti-CD19 CAR T cells for treating CLL patients.

## RESULTS

### Comparison of Hu19-CAR T cultured in IL-2 or IL-7+IL-15

The Hu19-CD828Z CAR used in this work was encoded by the mouse stem cell virus-based splice-gag vector (MSGV1).<sup>38</sup> Unmanipulated human PBMC were stimulated with an anti-CD3 monoclonal antibody added to culture media containing either IL-2 or IL-7+IL-15. On day 2 of culture, T cells were transduced with the MSGV1-Hu19-CD828Z gamma-retroviral vector. There was no statistically significant difference in CAR transduction efficiency for cells cultured in IL-2 or IL-7+IL-15 (Figure 1A). T cells can be divided into different memory subsets based on markers such as C-C chemokine receptor type 7 (CCR7), CD45RA, and CD95.<sup>39,40</sup> There was not a statistically significant difference in frequencies of CAR<sup>+</sup> central memory (CM) T cells (CD45RA-negative, CCR7<sup>+</sup>) when cultures supplemented with either IL-2 or IL-7+IL-15 were compared (Figure 1B). On day 7 of culture, there was a higher percentage of CD8<sup>+</sup> Hu19-CAR T with cell-surface markers of Tscm (CD45RA<sup>+</sup>CCR7<sup>+</sup>CD95<sup>+</sup>) for cultures with IL-7+IL-15 versus cultures with IL-2 (Figure 1C). An example of the raw flow cytometry data is presented in Figure S1. Note that one donor had Tscm levels substantially higher than the other donors (Figure 1C). The same donor also had the highest CM levels of all donors studied. Degranulation was assessed with a flow cytometry assay

for antigen-specific upregulation of CD107a. There was a slight but statistically higher level of degranulation for both CD4<sup>+</sup> and CD8<sup>+</sup> Hu19-CAR T cultured in IL-7+IL-15 versus IL-2 (Figure S2). Proliferation assays were conducted by culturing carboxyfluorescein diacetate succinimidyl ester (CFSE)-labeled Hu19-CAR T in cytokine-free medium with CD19<sup>+</sup> or CD19-negative target cells. When Hu19-CAR T generated in IL-2 or IL-7+IL-15 culture conditions were compared, no differences were observed in antigen-specific proliferation as assessed by CFSE dilution (Figure 1D), but the fold-increase in the number of Hu19-CAR T during the 4 days of co-culture with CD19<sup>+</sup> target cells was higher for Hu19-CAR T generated with IL-7+IL-15 versus IL-2 (Figure 1E). Hu19-CAR T cultured with either IL-2 or IL-7+IL-15 exhibited similar levels of antigen-specific interferon- $\gamma$  (IFN- $\gamma$ ) release (Figure 1F). Compared with Hu19-CAR T cells cultured with IL-2, Hu19-CAR T cultured with IL-7+IL-15 exhibited significantly higher levels of antigen-specific IL-2 release (Figure 1G).

Next, we evaluated whether Hu19-CAR T cultured with either IL-2 or IL-7+IL-15 had better anti-tumor outcomes in mice. Mice bearing palpable tumors of ST486 cells were treated with two different doses of Hu19-CAR T. In two separate mouse experiments, Hu19-CAR T anti-tumor activity was superior at higher cell doses (Figures 1H and 1I). There was not a statistically significant difference in tumor sizes or survival in mice treated with Hu19-CAR T cultured with IL-2 versus IL-7+IL-15 (Figures 1H and 1I). We decided to use IL-7+IL-15 to culture Hu19-CAR T in further studies because use of these cytokines was associated with higher levels of CD8<sup>+</sup> Tscm (Figure 1C), greater antigen-specific fold-increase in Hu19-CAR T numbers during proliferation assays (Figure 1E), and higher levels of IL-2 release (Figure 1G).

### Purification of T cells from PBMC

In CLL patients, the majority of blood lymphocytes are often leukemia cells.<sup>29</sup> Therefore, the purification of T cells is necessary prior to culture and transduction of T cells from CLL patients. To examine the most effective purification strategy, two primary methods were compared: CD19-depletion (19-dep) and CD4 plus CD8 positive selection (sel). For both methods, purification was done by magnetic-activated cell sorting (MACS). Due to the limited availability of CLL apheresis samples, we utilized PBMC from lymphoma patients in the experiments reported in Figures 2 and 3. These samples contained 10%–15% CD19<sup>+</sup> cells. T cell purity defined as the percentage of CD3<sup>+</sup> cells was higher after the sel method versus the 19-dep method (Figure 2A). The %CD3<sup>+</sup> T cell yield after purification was defined as the number of T cells present after purification divided by the number of T cells in PBMC before purification. The yield of T cells was similar with the sel and 19-dep methods (Figure 2B).

### Characteristics of Hu19-CAR T prepared by different methods

Cells purified by either the sel or 19-dep methods were individually activated with three different activating agents. Dynabeads (dyna) are paramagnetic beads expressing anti-CD3 and anti-CD28; dyna have commonly used in CAR T cell clinical manufacturing.<sup>16,41–43</sup> Transact (trans), a nanomatrix expressing anti-CD3 and anti-CD28,

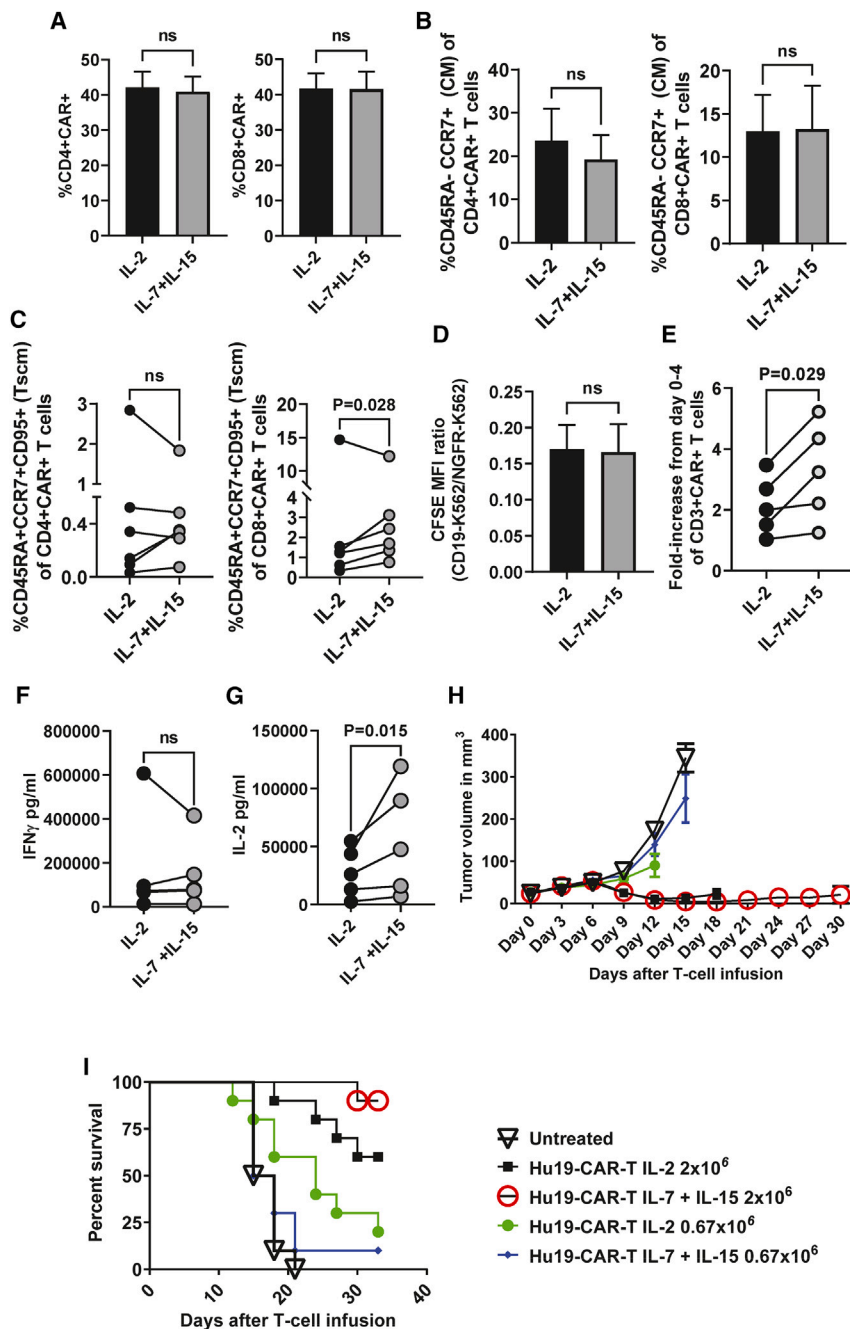


**Figure 1. Comparison of CAR T cultured in media containing IL-2 or IL-7+IL-15**

PBMCs were stimulated with anti-CD3 and cultured in media containing either IL-2 or IL-7+IL-15. After 2 days of culture, cells were transduced with MSGV1-Hu19-CD828Z. On day 7 of culture, flow cytometry was performed to assess CAR expression and memory phenotype. Plots were gated on live CD3<sup>+</sup> lymphocytes. Throughout, NS indicates no statistically significant difference, and  $p < 0.05$  was considered statistically significant. (A and B) Bars represent mean + SEM. (A) %CD4<sup>+</sup>CAR<sup>+</sup> (left) and %CD8<sup>+</sup>CAR<sup>+</sup> (right) of Hu19-CAR T cells. (B) Comparison of %CD45RA<sup>-</sup>CCR7<sup>+</sup> (CM) cells among CD4<sup>+</sup>CAR<sup>+</sup> (left) and CD8<sup>+</sup>CAR<sup>+</sup> (right) are shown. (C) Comparison of %CD45RA<sup>+</sup>CCR7<sup>+</sup>CD95<sup>+</sup> Tscm cells from CD4<sup>+</sup>CAR<sup>+</sup> (left) or CD8<sup>+</sup>CAR<sup>+</sup> (right) T cells cultured with different cytokines. (A–C)  $n = 6$ ; statistics were by paired, 2-tailed t test for (A) and (B) and ratio-paired, two-tailed t test for (C). (D and E) Proliferation was assessed. Hu19-CAR T were labeled with CFSE and cultured with either CD19-K562 cells or NGFR-K562 cells for 4 days. IL2 and IL-7+IL-15 refer to culture conditions before the proliferation assay. No cytokines were added to media of proliferation assays. (D) After 4 days of co-culture, CAR<sup>+</sup>CD3<sup>+</sup> live lymphocytes were assessed for the ratio of CFSE MFI of Hu19-CAR T after CD19-K562 co-culture versus NGFR-K562 co-culture (CFSE MFI ratio CD19-K562/NGFR-K562). Lower CFSE MFI ratios indicate more proliferation.  $n = 5$ . (E) There was a statistically higher fold-increase of CD3<sup>+</sup>CAR<sup>+</sup> cell numbers from day 0 to day 4 of co-culture with CD19-K562 for T cells cultured with IL-7+IL-15 versus IL-2;  $n = 5$ . (D and E) Statistics were by two-tailed paired t test. (F and G) Hu19-CAR T were co-cultured overnight with CD19-K562 or NGFR-K562 cells, and ELISA was performed on supernatants (F) IFN- $\gamma$  and (G) IL-2. There was a statistically significant difference in IL-2 production between IL-7+IL-15 versus IL-2 conditions. For F–G,  $n = 5$ , statistics were by two-tailed ratio paired t test. (H and I) ST486 solid tumors were established in NSG mice. Six days after tumor implantation, mice were left untreated or received infusions of either  $0.67 \times 10^6$  or  $2 \times 10^6$  Hu19-CAR T cultured in IL-2 or IL-7+IL-15. (H) Graph shows mean tumor volume  $\pm$  SEM for each time point. The graph shows combined data from two experiments performed with cells from different donors;  $n = 10$  mice per treatment group. (I) Survival of mice from (H). By log rank test, there was no statistically significant differences in survival between mice receiving Hu19-CAR T cultured in IL-2 or IL-7+IL-15. There was a statistically significant difference in survival between mice receiving  $2 \times 10^6$  versus  $0.67 \times 10^6$  Hu19-CAR T cultured in IL-2 ( $p = 0.048$ ), and there was a statistically significant difference in survival between mice receiving  $2 \times 10^6$  versus  $0.67 \times 10^6$  Hu19-CAR T cultured in IL-7+IL-15 ( $p < 0.0001$ ). The legend defines which symbols represent each treatment group in (H) and (I).

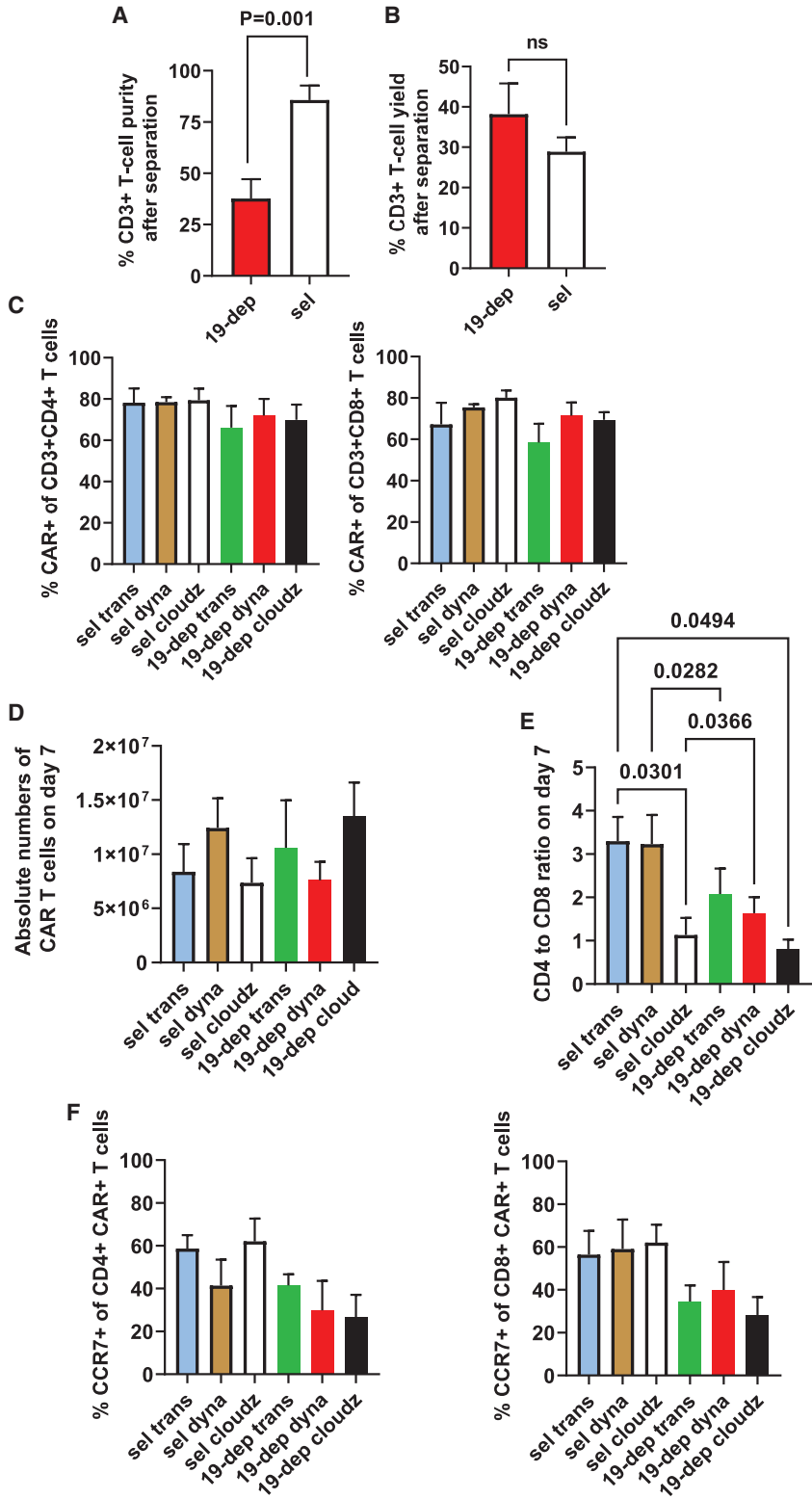
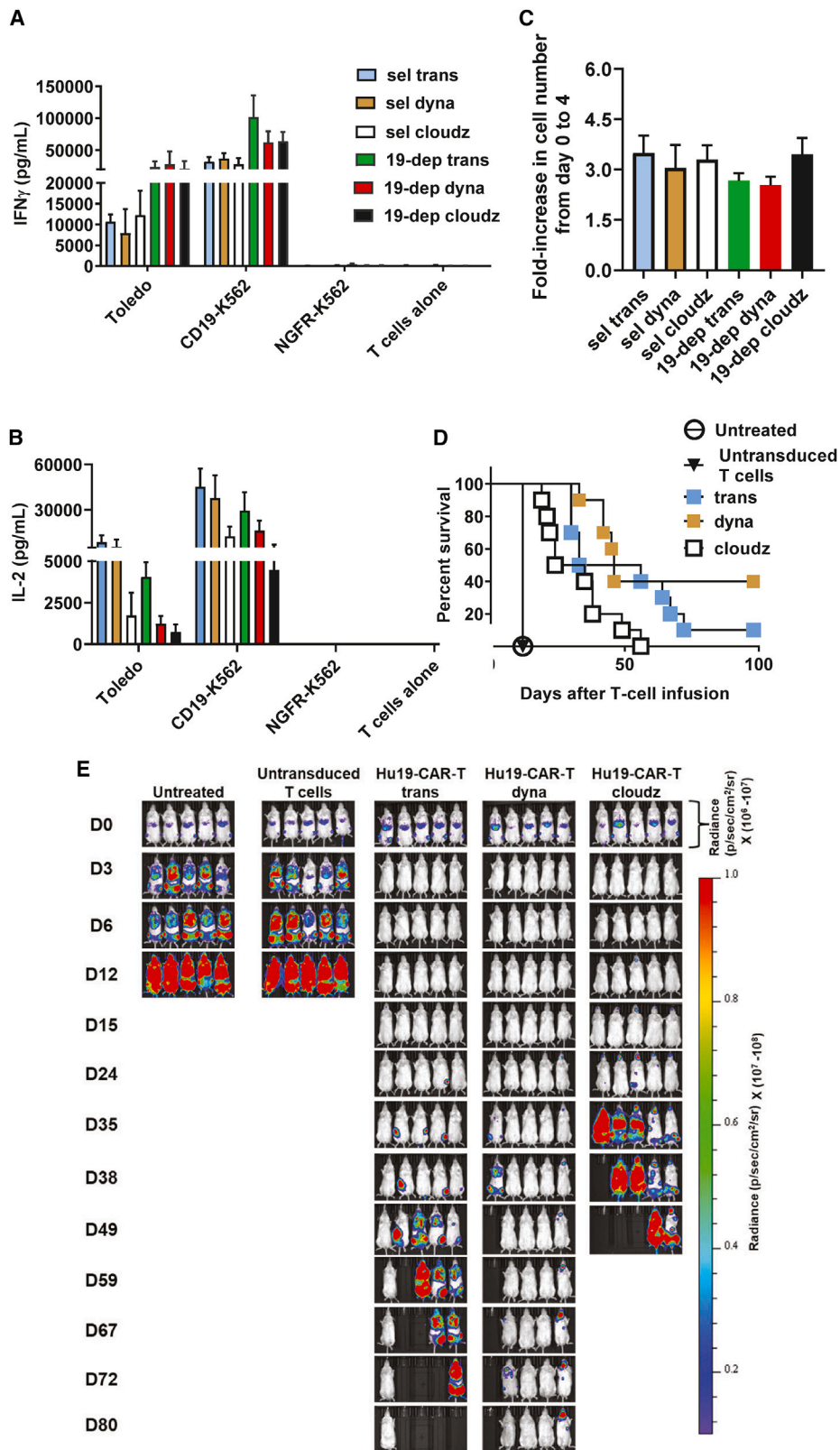


**Figure 2. Comparison of T cell purification methods**

Throughout Figure 2, bar graphs are mean + SEM. For the 19-dep method, PBMCs were labeled with anti-CD19 microbeads and CD19<sup>+</sup> cells were depleted (19-dep). For the T cell selection (sel) method, PBMCs were separately labeled with either anti-CD4 or anti-CD8 microbeads. CD4<sup>+</sup> and CD8<sup>+</sup> T cells were positively selected and then combined as one T cell fraction. (A) Bar graphs represent %CD3<sup>+</sup> T cells as determined by flow cytometry after 19-dep or sel T cell purification. There was a statistically higher %CD3<sup>+</sup> cells with the sel method compared with the 19-dep method; n = 4. (B) Bars represent %CD3<sup>+</sup> T cell yield after purification. %CD3<sup>+</sup> T cell yield was calculated by dividing the post-purification T cell count by the pre-purification T cell count; n = 4. Statistical testing was by paired, two-tailed t tests for (A and B). ns, not statistically significant. (C–F) Cells purified by the 19-dep or sel methods were separately divided into three portions. Each cell portion was activated with trans, dyna, or cloudz. Activated cells from each method were transduced with the gene for the Hu19-CD828Z CAR. On day 7 of T cell cultures, live transduced cells were stained for CD3, CD4, CD8, CAR, CD45RA, CCR7, and CD95. (C) Bars represent %CAR<sup>+</sup> T cells among CD3<sup>+</sup>CD4<sup>+</sup> T cells (left) and CD3<sup>+</sup>CD8<sup>+</sup> T cells (right). For both CD4<sup>+</sup> and CD8<sup>+</sup> T cells, there was no statistically significant difference in CAR expression. (D) Graph shows the absolute number of CAR<sup>+</sup> T cells on day 7 of culture. CAR<sup>+</sup> T cell numbers were determined by multiplying the cell count by the %CD3<sup>+</sup>CAR<sup>+</sup> determined by flow cytometry. There was no statistically significant difference in the number of CAR<sup>+</sup> cells between different groups. (E) Graph shows CD4:CD8 ratios of CD3<sup>+</sup>CAR<sup>+</sup> cells produced by different methods; all statistically significant differences are noted on the figure. (C–E) n = 4 different donors. (F) Comparison of %CCR7<sup>+</sup> of CD3<sup>+</sup>CAR<sup>+</sup> cells that were either CD4<sup>+</sup> (left) or CD8<sup>+</sup> (right). For both CAR<sup>+</sup>CD4<sup>+</sup> and CAR<sup>+</sup>CD8<sup>+</sup> T cells, there were not statistically significant differences in %CCR7<sup>+</sup> between the different methods; n = 3. Statistical testing was by repeated-measures one-way ANOVA with Tukey's multiple comparisons test for (C–F). Statistical significance was defined as p < 0.05 for the entire figure.



(legend on next page)

has been used a clinical trial.<sup>44,45</sup> Cloudz consists of dissolvable microspheres expressing anti-CD3 and anti-CD28.<sup>46</sup> All T cell cultures described in the rest of this report were supplemented with IL-7+IL-15. There were no statistically significant differences in CAR expression among CD4 or CD8 T cells for the different Hu19-CAR T preparation methods (Figure 2C). Similarly, there were no statistically significant differences in the absolute numbers of CAR T cells on day 7 of culture between the different Hu19-CAR T preparation methods (Figure 2D). T cell activation with the cloudz reagent generally led to Hu19-CAR T with a lower CD4:CD8 ratio on day 7 (Figure 2E). There was also a trend toward a lower CD4:CD8 ratios with the 19-dep method. The total percent CCR7<sup>+</sup> T cells was evaluated as an indicator of less differentiated cells.<sup>40</sup> There was an overall trend toward higher %CCR7<sup>+</sup> with sel-derived Hu19-CAR T cells compared with 19-dep-derived Hu19-CAR T (Figure 2F). This trend did not reach statistical significance.

We evaluated the anti-CD3/CD28 dyna T cell enrichment method, which has been used to enrich T cells from total PBMCs for clinical CAR T cell production.<sup>16,28,43</sup> We purified CLL PBMC with high percentages of CD19<sup>+</sup> leukemic cells. When compared with the dyna enrichment method, the sel method had superior T cell purity and CD19<sup>+</sup> leukemic cell depletion on days 0 and 2 of culture (Figure S3A). However, by day 7 of culture, both cultures exhibited similar percentages of CD3<sup>+</sup> T cells. CAR expression on T cells derived from either the sel or dyna-enrichment methods was comparable (Figure S3B). The %CCR7<sup>+</sup> Hu19-CAR T cells was similar for either the sel or dyna-enrichment methods (Figure S3C). Higher numbers of Hu19-CAR T were generated in cultures after sel versus dyna enrichment (Figure S3D). Because of the lower purity of T cells on day 2 of culture (Figure S3A) and the lower number of Hu19-CAR T generated by day 7 with the dyna-enrichment method versus the sel method (Figure S3D), we did not further test the dyna-enrichment method.

#### Comparison of Hu19-CAR T function with different preparation approaches

Antigen-specific Hu19-CAR T function was assessed by co-culture with CD19<sup>+</sup> or CD19-negative target cells followed by assays. We did not observe any statistically significant differences across the

tested Hu19-CAR T preparation approaches for IFN- $\gamma$  and IL-2 release (Figures 3A and 3B), CD107a surface expression (Figure S4), and antigen-specific increases in cell number during proliferation assays (Figure 3C). However, there were trends toward higher IFN- $\gamma$  production with cells derived from the 19-dep method and increased IL-2 production with cells derived from the sel method; these trends did not reach statistical significance. Overall, the data demonstrated similar characteristics of Hu19-CAR T produced with either the 19-dep or sel methods regardless of activating agents except the cloudz reagent generated Hu19-CAR T with a lower CD4:CD8 ratio. The sel method exhibited superior T cell purity (Figure 2A) as well as trends toward a higher percent of CCR7<sup>+</sup> CAR T cells (Figure 2F) and higher IL-2 release (Figure 3B). Therefore, we decided to proceed with the sel method to purify T cells from CLL PBMC for further testing.

#### In vivo anti-tumor activity of Hu19-CAR T generated by different methods

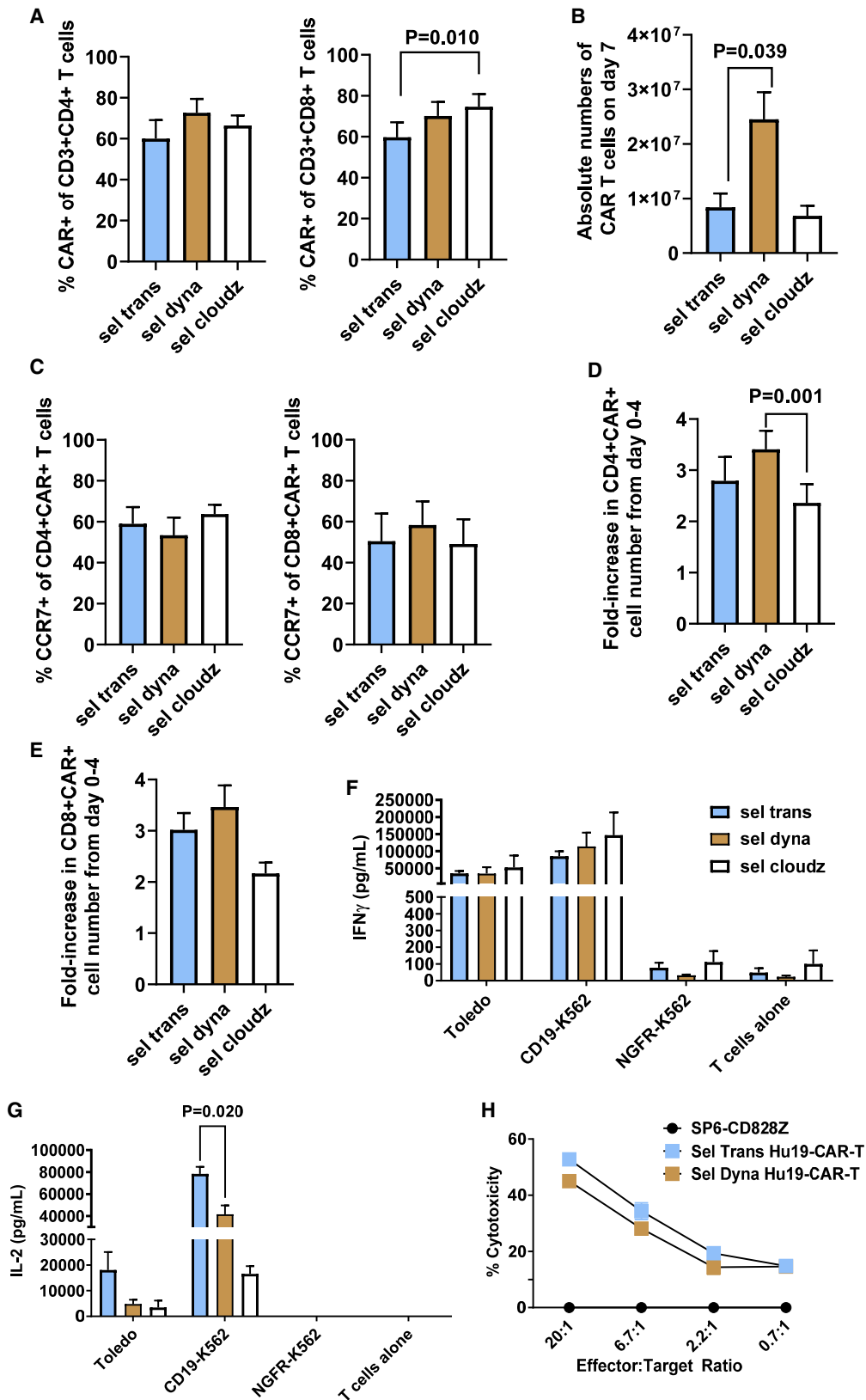
Disseminated NALM6-GL cells were established in nod-scid common  $\gamma$ -chain knockout mice (NSG, NOD.Cg-Prkdc<sup>scid</sup> Il2rg<sup>tm1Wjl/SzJ</sup>). Mice were treated with sel-derived Hu19-CAR T that were activated with trans, dyna or cloudz. Mice treated with Hu19-CAR T activated with cloudz consistently exhibited inferior anti-leukemia activity compared with mice treated with Hu19-CAR T activated by the other approaches (Figures 3D and 3E). There was not a statistically significant difference in survival between mice treated with Hu19-CAR T produced by activation with trans versus activation with dyna, but 4 of 10 mice treated with dyna-activated Hu19-CAR T were alive at the end of the experiments while only 1 of 10 mice treated with trans-activated Hu19-CAR T were alive at the end of the experiments (Figure 3D). Dyna-activated versus trans-activated Hu19-CAR T were associated with slightly more sustained leukemia clearance (Figures 3E and S5A), but on the last days when all mice were alive and able to be accurately imaged, the mean bioluminescence intensity was statistically lower for dyna-activated versus trans-activated Hu19-CAR T in only one of the two experiments (Figure S5B).

#### Assessment of Hu19-CAR T derived from PBMC of CLL patients

In the experiments shown in Figures 4A–4E, we utilized PBMC from three CLL patients to evaluate the sel method with the three activating

#### Figure 3. Function of Hu19-CAR T produced with different methods

(A and B) T cells prepared by the six different approaches shown in the legend were cultured overnight alone or with target cells. Toledo and CD19-K562 target cells were CD19<sup>+</sup>; NGFR-K562 cells were CD19-negative. After overnight culture, culture supernatant was assayed by ELISA for (A) IFN- $\gamma$  and (B) IL-2. For (A) and (B), bars represent mean + SEM cytokine levels; n = 4 except for Toledo, which had n = 3. different donors. There were no statistically significant differences between the methods for either IFN- $\gamma$  or IL-2. Statistical testing was by repeated-measures one-way ANOVA. For this entire figure, p < 0.05 was considered statistically significant. (C) CD19-specific CFSE proliferation assay was performed. Bars represent mean + SEM fold-increase of the absolute number of CAR<sup>+</sup>CD3<sup>+</sup> cells from day 0 to day 4 of culture; n = 4 different donors. There were not statistically significant differences when the six groups were compared. Statistical testing was repeated-measures one-way ANOVA. (D and E) Mice were treated with Hu19-CAR T activated with trans, dyna, or cloudz according to the legend in (D). For all groups, T cells were purified by positive selection (sel). NALM6-GL leukemia cells were established by intravenous injection of  $2 \times 10^6$  NALM6-GL cells into NSG mice 3 days prior to CAR T cell infusions. Mice were either untreated or received infusions of either  $8 \times 10^6$  Hu19-CAR T or untransduced T cells. (D) Kaplan-Meier percent survival graph of the mice treated with different CAR T cell cultures. By the log rank test, there were statistically significant differences in percent survival between cloudz versus dyna (p = 0.006) and cloudz versus trans (p = 0.032) groups. There was no statistically significant difference in percent survival between dyna and trans groups. The survival curve contains data from two experiments with different donors. N = 10 total mice per group. (E) The figure shows bioluminescence (BLI) intensity of mice for each time point. BLI radiance scale of  $\times 10^6$ - $10^7$  radiance was used for day 0 images and  $\times 10^7$ - $10^8$  radiance was used for all images starting at day 3. There was not a statistically significant difference in mean BLI between the trans and dyna groups at the last time point when all mice in both groups were alive.



(legend on next page)

agents. The three CLL samples had 34.5%, 36.9%, and 25.0% CD20<sup>+</sup> cells. CLL PBMCs were also used to conduct the other experiments shown in Figure 4. There were no statistically significant differences in transduction efficiency between the different T cell-activating reagents for CD3<sup>+</sup>CD4<sup>+</sup> cells, but for CD3<sup>+</sup>CD8<sup>+</sup> cells, there was a statistically higher transduction efficiency for cloudz versus trans (Figure 4A). There was not a statistically significant difference in the CD4:CD8 ratio for the different activation agents, but there was a trend toward a lower CD4:CD8 ratio for cloudz (Figure S6A). Aside from a statistically higher degranulation of CD4<sup>+</sup> Hu19-CAR T for trans versus dyna, there were no differences in degranulation measured by CD107a upregulation for the different activation methods (Figure S6B). By day 7 of Hu19-CAR T production, higher numbers of CAR<sup>+</sup> T cells accumulated with dyna activation compared with trans activation (Figure 4B). There were no statistically significant differences in %CCR7 for either CD4<sup>+</sup>CAR<sup>+</sup> or CD8<sup>+</sup>CAR<sup>+</sup> T cells when the different T cell-activating reagents were compared (Figure 4C). During proliferation assays, there was a greater antigen-specific fold-increase in CD4<sup>+</sup> Hu19-CAR T with dyna activation than with cloudz activation (Figure 4D), and there was a trend toward greater fold-increase in CD8<sup>+</sup> Hu19-CAR T with dyna versus cloudz activation (Figure 4E). There were no statistically significant differences among the activating agents for T cell proliferation measured by CFSE dilution (Figure S6C). There were no statistically significant differences in IFN- $\gamma$  release among Hu19-CAR T produced with the different T cell activation methods (Figure 4F). IL-2 release after overnight co-culture of Hu19-CAR T with CD19-K562 target cells was higher with trans activation than dyna activation (Figure 4G). Hu19-CAR T produced with trans or dyna were equally capable of inducing cytotoxicity against autologous primary CLL cells (Figure 4H). Hu19-CAR T products produced with either dyna or trans activation were similar. We chose to use dyna activation for clinical Hu19-CAR T production because higher numbers of Hu19-CAR T accumulated by day 7 of Hu19-CAR T production cultures for dyna versus trans (Figure 4B). In addition, there was a trend, which was not statistically significant, toward better *in vivo* tumor elimination for dyna versus trans activation (Figures 3D, 3E, and Figure S5).

#### Rtx did not impact anti-tumor efficacy of Hu19-CAR T

We assessed the impact of Rtx treatment on Hu19-CAR T anti-tumor activity with two different tumor models (Figure 5A). In these experiments, Rtx was administered three times per week over the 30 days after Hu19-CAR T infusion. NALM6-GL cells are CD19<sup>+</sup>CD20<sup>+</sup>. In a disseminated NALM6-GL model, Rtx treatment as described in Figure 5A did not affect anti-tumor efficacy of Hu19-CAR T (Figures 5B and 5C). ST486 cells are CD19<sup>low</sup>CD20<sup>hi</sup>. ST486 tumor-bearing mice were treated as described in Figure 5A. Rtx neither impaired nor improved anti-tumor efficacy of Hu19-CAR T against ST486 tumors when a dose of  $2 \times 10^6$  Hu19-CAR T per mouse was administered (Figures 5D and 5E). Hu19-CAR T alone at a dose of  $2 \times 10^6$  Hu19-CAR T per mouse had superior anti-tumor activity when compared with Rtx alone (Figures 5D and 5E). We also assessed a lower dose of  $1 \times 10^6$  Hu19-CAR T per mouse in combination with Rtx. With this lower dose of Hu19-CAR T, Hu19-CAR T + Rtx had superior anti-tumor activity than Hu19-CAR T cells + control immunoglobulin. In addition, Hu19-CAR T cells + Rtx had superior anti-tumor activity when compared with Rtx only (Figure S7).

#### Good manufacturing practices-compatible Hu19-CAR T manufacturing process for CLL patients

After assessing different cell production parameters, we next developed a good manufacturing practices (GMP)-compatible Hu19-CAR T production process for clinical use. The entire project to develop this process is summarized in Figure S8. The clinical manufacturing process that was selected includes CD4 plus CD8 positive selection, dyna activation, and culture with IL-7+IL-15 (Figure 6A). In the clinical Hu19-CAR T preparation plan, T cells were purified from starting PBMC with the CliniMACS Plus system. Subsequent T cell activation and gamma-retroviral transduction and cell culture were performed in cell culture bags. A summary of product release safety criteria for the clinical Hu19-CAR T, including microbiology tests, endotoxin, replication-competent retrovirus testing, vector transgene copy number, and bead detection for three GMP-compatible test Hu19-CAR T productions, are presented in Table S1. The clinical T cell purification process eliminated most CD19<sup>+</sup> B cells from CLL PBMC (Figure 6B) and resulted in a

#### Figure 4. *In vitro* assessment of Hu19-CAR T derived from CLL PBMC

The positive selection (sel) method was used to obtain T cells from CLL PBMC. The selected cells were activated independently with trans, dyna, or cloudz on day 0. The activated cells were transduced with MSGV1-Hu19-CD828Z. (A–E) Bars represent mean + SEM, n = 3 different CLL donors. (A–E) Statistical testing was done by repeated-measures one-way ANOVA with Tukey's multiple comparisons test; p < 0.05 was considered statistically significant. Experiments in A–C were performed on day 7 of culture. (A) Graphs show %CAR<sup>+</sup> T cells among cells gated on live CD3<sup>+</sup>CD4<sup>+</sup> T cells (left) or live CD3<sup>+</sup>CD8<sup>+</sup> T cells (right). For both CD4<sup>+</sup> and CD8<sup>+</sup> T cells, there was no statistical difference in the CAR expression between the different activation methods except between trans and cloudz for CD8<sup>+</sup> cells. (B) Absolute number of accumulated Hu19-CAR T on day 7 of culture with the different activation methods. There was a statistically significant difference in the accumulated number of CAR T cells activated with trans versus dyna. (C) Comparison of the percentages of CAR<sup>+</sup> T cells that were CCR7<sup>+</sup> for CD4<sup>+</sup> (left) or CD8<sup>+</sup> (right) T cells. There was no statistically significant difference between the groups. (D) CD19-specific CFSE proliferation assays were performed. The fold-increases of T cells during the 4-day culture are shown for CAR<sup>+</sup>CD4<sup>+</sup> T cells. There was a statistically significant difference in the fold-increase between T cells activated with dyna versus cloudz. (E) The fold-increases of CAR<sup>+</sup>CD8<sup>+</sup> T cells in CFSE assays are shown; there were no statistically significant differences between groups. (F and G) On day 9 of the T cell culture, Hu19-CAR T were co-cultured overnight alone or with Toledo, CD19-K562 or NGFR-K562 cells. After the co-culture, supernatants were assayed for (F) IFN- $\gamma$  or (G) IL-2. (F and G) Bars represent mean + SEM, n = 4 different CLL donors except cloudz, which had n = 3. Statistical testing was by mixed-effects analysis with Tukey's multiple comparisons test. There was no statistically significant difference in IFN- $\gamma$  release between the T cell activation methods. There was a statistically significant difference in IL-2 release for trans versus dyna. (H) A 4-h cytotoxicity assay was performed by co-culturing Hu19-CAR T with autologous CLL target cells at the indicated effector:target ratios. The positive target cells were CLL PBMC containing 85.7% CD20<sup>+</sup> cells. Mean  $\pm$  SEM of %cytotoxicity in duplicate wells is graphed. The experiment was conducted two times with cells from different donors with similar results.

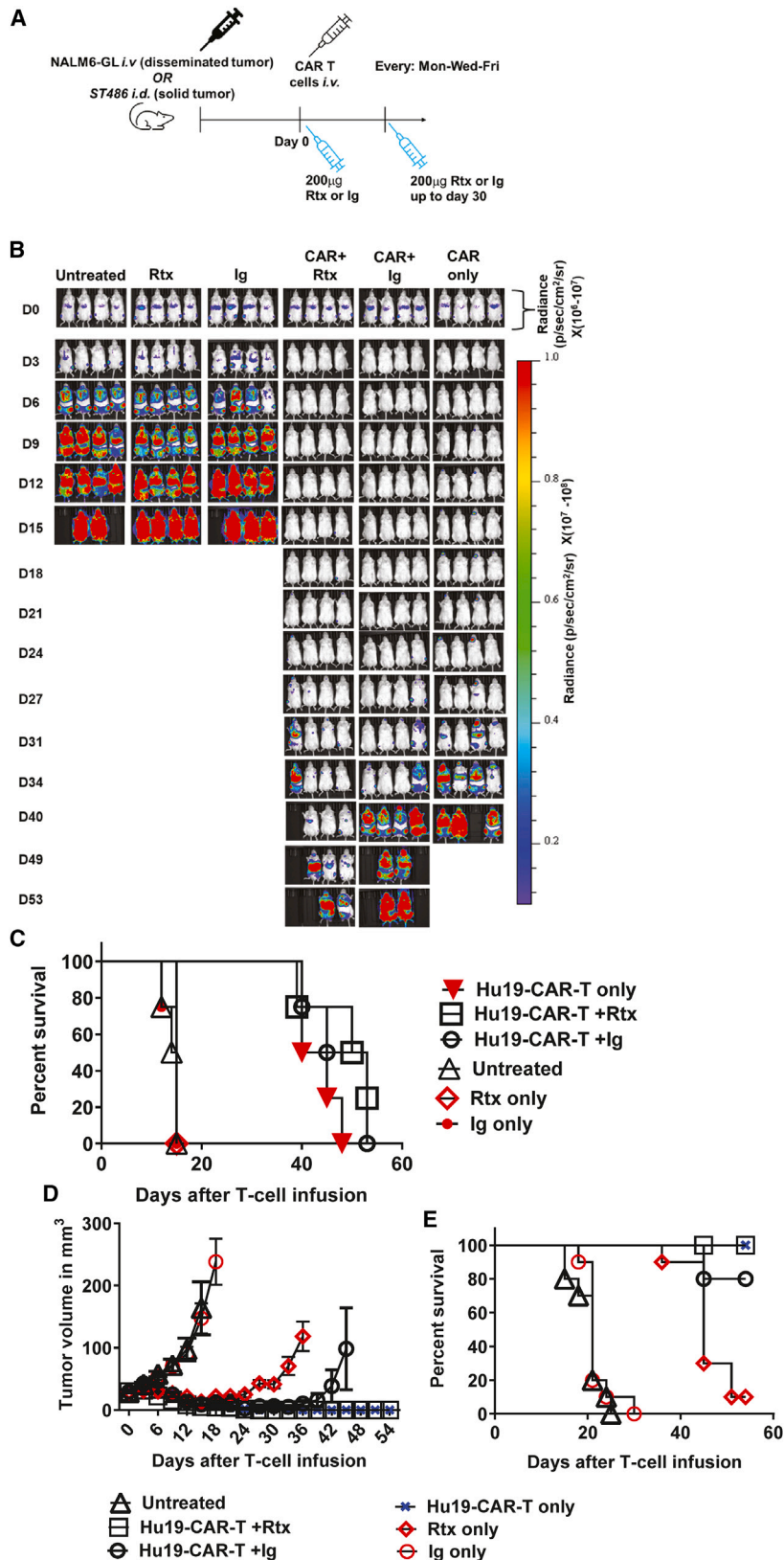
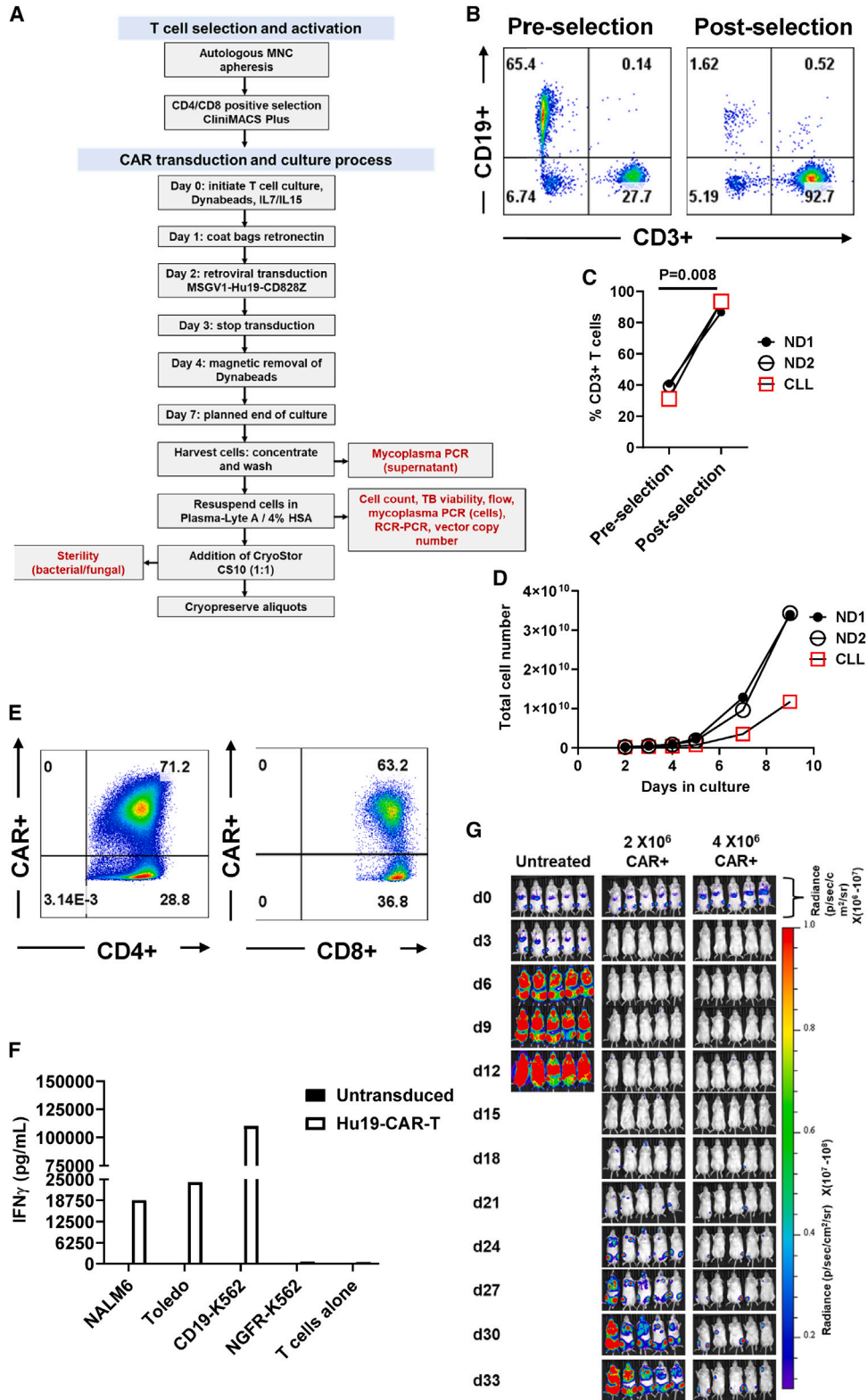


**Figure 5. Effects of Rtx on anti-tumor activity of Hu19-CAR T**

(A) Schematic of NALM6-GL and ST486 tumor models with Rtx treatment. Dispersed NALM6-GL was established via intravenous (i.v.) injection. ST486 solid tumors were established by intradermal (i.d.) injection. Starting on the day of Hu19-CAR T infusion (day 0), some groups of mice received intraperitoneal injections of either 200 µg Rtx or 200 µg normal human IgG (Ig) control antibody every Monday, Wednesday, and Friday up to day 30 after Hu19-CAR T infusion. (B) Dispersed NALM6-GL leukemia cells were established in mice by injecting  $2 \times 10^6$  NALM6-GL cells. Three days later, groups of four mice each were left untreated or treated with Rtx only, Ig only, Hu19-CAR T + Rtx, Hu19-CAR T + Ig, or Hu19-CAR T only. A dose of  $8 \times 10^6$  Hu19-CAR T per mouse was used. In the figure, CAR refers to Hu19-CAR T. Bioluminescence (BLI) intensity of different groups is shown for each time point. BLI radiance scale of  $\times 10^6-10^7$  was used for day 0 images, and BLI radiance scale of  $\times 10^7-10^8$  was used for all the images day 3 or later. (C) Kaplan-Meier percent survival graph of the same mice as in (B). By the log rank test, there was not a statistically significant difference in survival for any comparison among the Hu19-CAR T + Rtx, Hu19-CAR T + Ig, and Hu19-CAR T only groups. There were statistically significant differences between Rtx only versus Hu19-CAR T + Rtx, Rtx only versus Hu19-CAR T + Ig, and Rtx only versus Hu19-CAR T only ( $p = 0.0082$  for all 3 comparisons);  $n = 4$ , mice per group. (D) ST486 solid tumors were established, and mice were left untreated or treated with Hu19-CAR T + Rtx, Hu19-CAR T + Ig, Hu19-CAR T only, Rtx only, or Ig only. Tumor volumes are shown. Day 0 is the day of infusion of  $2 \times 10^6$  Hu19-CAR T cells. (E) Kaplan-Meier survival graph of the same mice as in (D). By the log rank test, there was not a statistically significant difference in survival for any comparison among the Hu19-CAR T + Rtx, Hu19-CAR T + Ig and Hu19-CAR T only groups. There were statistically significant differences between Rtx only versus Hu19-CAR T + Rtx ( $p < 0.0001$ ), Rtx only versus Hu19-CAR T + Ig ( $p = 0.0021$ ), and Rtx only versus Hu19-CAR T only ( $p = 0.0021$ ). For (D) and (E),  $n = 10$  mice per treatment group except for Hu19-CAR T cells only, which had 5 mice. (D and E) Combined data from two independent experiments with different donors.



(legend on next page)

statistically significant increase in T cell purity (Figure 6C). Figure 6D shows the rate of accumulation of Hu19-CAR T during the clinical cell culture process. Cells were transduced on day 2 of culture and were counted at the time-points indicated on the x axis.

Hu19-CAR T derived from CLL donor PBMC by the clinical cell production process had high levels of CAR expression (Figure 6E), and these Hu19-CAR T exhibited CD19-specific release of IFN- $\gamma$  (Figure 6F) and IL-2 (Figure S9A). Hu19-CAR T derived from CLL PBMC by the clinical production process eliminated NALM6-GL cells from mice. There was a dose-dependent anti-tumor response, with better tumor clearance and survival at a  $4 \times 10^6$  Hu19-CAR T dose compared with a  $2 \times 10^6$  Hu19-CAR T dose (Figures 6G and S9B).

## DISCUSSION

CLL consists of clonal B cells that accumulate in the bone marrow, blood, spleen, and lymph nodes of patients. Contact with CLL B cells can lead to adverse changes in T cells, including the expression of phenotypic markers of exhaustion and functional defects.<sup>30,31,47,48</sup> In addition to these reported defects in T cells from CLL patients, CD19<sup>+</sup> CLL cells contaminating cell cultures during production of Hu19-CAR T might lead to activation-induced cell death (AICD) via the mechanism of repeated stimulation of the anti-CD19 CAR by its target antigen as has been shown for CARs targeting solid tumors.<sup>49,50</sup> Because of the potentially high levels of leukemia cells in CLL patient PBMC (Figure S3A), we evaluated three different methods of purifying T cells from PBMC, sel, 19-dep, and dyna enrichment. T cell purity was higher for the sel method versus the dyna-enrichment method (Figure S3A). Additionally, the sel method yielded higher T cell purity than the 19-dep method (Figure 2A). There was a trend that was not statistically significant toward higher CCR7<sup>+</sup> Hu19-CAR T with sel versus 19-dep (Figure 2F). Based on greater T cell purity, we selected the sel method of purification.

The second aspect of Hu19-CAR T cells production that we evaluated was the T cell activation reagent. Cloudz was formerly available in a GMP-compliant format that has been discontinued, which makes it impossible to use this reagent in any future clinical trial. There was a

consistently lower CD4:CD8 ratio with cloudz compared with the other T cell activation reagents (Figure 2E). Our results showed that Hu19-CAR T produced with cloudz were inferior Hu19-CAR T produced with dyna or trans at eliminating leukemia from mice (Figure 3).

Prior investigators have compared dyna and trans. A study by Noaks et al.<sup>51</sup> found that monocytes affected activation by trans less than activation by dyna. Arcangeli et al.<sup>52</sup> demonstrated that CAR T-cells produced from healthy donor PBMC had similar phenotypic and functional characteristics after activation with either dyna or trans. For the most part, we agree with the results of Arcangeli et al.,<sup>52</sup> but we did find some advantages for dyna. Greater CAR T cell accumulation in culture during CAR T cell production from CLL PBMC has been associated with higher peak blood CAR gene copy numbers and with better anti-leukemia outcomes.<sup>32</sup> In our experiments, greater numbers of Hu19-CAR T accumulated by day 7 of cultures activated with dyna compared with trans during Hu19-CAR T production from CLL PBMC (Figure 4B). In addition, there was a trend toward better *in vivo* anti-leukemia activity for dyna activation compared with trans activation; however, the differences in anti-leukemia activity only reached statistical significance for 1 of 2 experiments (Figures 3D, 3E, and S5). We selected dyna as the T cell-activating reagent for our clinical Hu19-CAR T production process.

Higher peak blood CAR T cell levels in the blood of patients have been associated with better anti-malignancy responses in CLL and other hematological malignancies,<sup>32,53–55</sup> and less differentiated infused CAR T cells have been associated with higher peak blood CAR<sup>+</sup> cell levels.<sup>34,53</sup> Less-differentiated T cells have been shown to be superior to highly differentiated T cell at treating tumors in mice,<sup>56,57</sup> and some evidence exists for less-differentiated T cells being more effective than highly differentiated T cells, such as exhausted T cells, at treating malignancy in humans.<sup>32,55,58,59</sup> Taken together, these findings suggest that generating CAR T cells with a less differentiated phenotype, which is associated with markers such as CD62L and CCR7, is preferable.

Our results showed that the percentage of CD8<sup>+</sup> Hu19-CAR T that had a Tscm phenotype was higher with culture in IL-7+IL-15 versus

### Figure 6. GMP-compatible manufacturing of Hu19-CAR T cells from CLL PBMC

(A) Schema of Hu19-CAR T clinical manufacturing is shown. T cells were purified from PBMCs of CLL patients by using CD4 plus CD8-positive selection with a CliniMACS Plus system. The separated cells were activated with anti-CD3/CD28 dyna and cultured in media with IL-7+IL-15. T cells were transduced with GMP-compliant MSGV1-Hu19-CD828Z vector. The total culture period for Hu19-CAR T was 7 days. Hu19-CAR T end-of-production testing and cryopreservation are included on the schema. TB stands for trypan blue. Results described in (B–G) are from Hu19-CAR T prepared by using the clinical preparation process shown in A. (B) Plots show %CD19<sup>+</sup> cells and %CD3<sup>+</sup> T cells before and after CD4 plus CD8 positive selection performed on PBMCs from a CLL patient. (C) %CD3<sup>+</sup> T cells before and after CD4 plus CD8 positive selection performed on PBMCs from two normal donors (NDs) and a CLL donor. There was a statistically significant difference between pre-selection and post-selection %CD3<sup>+</sup> T cells by two-tailed, paired t test;  $p < 0.05$  was considered statistically significant. (D) Accumulation of Hu19-CAR T from days 2 to 9 of the cell production process depicted in (A). (E) Flow plots show CD4<sup>+</sup>CAR<sup>+</sup> and CD8<sup>+</sup>CAR<sup>+</sup> T cells derived from CLL PBMCs. Cells were analyzed on day 7 of the clinical manufacturing process. Plots are gated on CD3<sup>+</sup> live lymphocytes and further gated on either CD4<sup>+</sup> or CD8<sup>+</sup> cells. (F) On day 7 of clinical manufacturing, Hu19-CAR T derived from CLL PBMC were cultured alone or co-cultured with CD19-positive (NALM6, Toledo, CD19-K562) or CD19-negative (NGFR-K562) target cells. After overnight culture, supernatants were assayed for IFN- $\gamma$  production. Bars are not visible for NGFR-K562 and T cells alone because of low levels of IFN- $\gamma$  release. (G). Disseminated NALM6-GL cells were established. On day 0, mice were left untreated or injected intravenously with either  $2 \times 10^6$  or  $4 \times 10^6$  Hu19-CAR T derived from a CLL donor's PBMCs according to the schema shown in (A). The figure shows the BLI of different groups of mice for each time point. A BLI-radiance scale of  $\times 10^6$ – $10^7$  was used for day 0 images and BLI-radiance scale of  $\times 10^7$ – $10^8$  radiance was used for images day 3 or later. N = 5 mice per group.

IL-2 (Figure 1C). Two other findings led us to select IL-7+IL-15 for Hu19-CAR T cell cultures. There was a greater fold increase in Hu19-CAR T numbers in proliferation assays (Figure 1E) and greater antigen-specific IL-2 release by Hu19-CAR T (Figure 1G) cultured in IL-7+IL-15 versus IL-2. We did not see an *in vivo* advantage for IL-7+IL-15 versus IL-2 in the mouse model that we used (Figures 1H and 1I). We think the advantages of IL-7+IL-15 versus IL-2 for cell culture are quite subtle; however, given the modest advantages of IL-7+IL-15 versus IL-2 *in vitro*, we believe further study is warranted.

In a planned clinical trial, we will administer the anti-CD20 monoclonal antibody Rtx prior to apheresis performed to collect PBMC of CLL patients. We also plan to administer a second dose of Rtx with a fludarabine plus cyclophosphamide conditioning regimen given before Hu19-CAR T infusion. There are three rationales for administering Rtx. First, CLL expresses CD20,<sup>19</sup> and Rtx has activity against CLL.<sup>5,6</sup> Second, administering Rtx prior to apheresis will reduce CLL cells in the apheresis PBMC. This will facilitate obtaining a highly pure T cell population after CD4 plus CD8-positive selection, which is the first step in Hu19-CAR T production. Highly pure starting T cells might prevent contaminating CLL cells from causing Hu19-CAR T exhaustion and AICD during Hu19-CAR T production.<sup>30,31,47,50</sup> Third, Rtx will contribute to reducing the CLL burden in patients prior to infusion of Hu19-CAR T. Since cytokine release syndrome and CAR-associated neurotoxicity are associated with malignancy burden,<sup>60</sup> administering Rtx might reduce the toxicity associated with Hu19-CAR T because Rtx can reduce the CLL burdens in patients.<sup>5,6</sup> In murine experiments, Rtx neither inhibited nor enhanced the treatment of NALM6-GL leukemia by Hu19-CAR T (Figures 5B and 5C). Rtx also did not inhibit or enhance treatment of solid tumors of ST486 cells with a Hu19-CAR T dose of  $2 \times 10^6$  cells/mouse (Figures 5D and 5E), but with a lower dose of  $1 \times 10^6$  Hu19-CAR T, Rtx plus Hu19-CAR T had superior anti-tumor activity versus control IgG plus Hu19-CAR T (Figure S7). Of note, antibody-mediated B cell depletion prior to or during adoptive T cell therapy was shown to enhance CAR T cell efficacy in other preclinical models.<sup>61,62</sup>

Changes in cell production processes could affect toxicity experienced by patients after CAR T cell infusion, but how changes in CAR T cell production will affect toxicity is difficult to predict from preclinical experiments. One possible indicator of clinical toxicity is the production of inflammatory cytokines by CAR T cells.<sup>63</sup> We did not see statistically different levels of IFN- $\gamma$  release by CAR T cells when cell production parameters were compared. We did see an increase in IL-2 release by CAR T cells cultured with IL-7+IL-15 versus IL-2 (Figure 1G).

For our clinical Hu19-CAR T production protocol, we utilized the CliniMACS Plus system for T cell purification (Figure 6A). All subsequent steps including T cell activation, gamma-retroviral transduction, and T cell culture were carried out in cell-culture bags. When the CliniMACS Prodigy was used to transduce T cells with a gamma-retroviral vector encoding a bicistronic anti-CD19/CD22

CAR construct, there was a low median percent CAR<sup>+</sup> T cells of 17.7% in a recent clinical trial.<sup>44</sup> This finding and our own prior experience suggested that transduction in cell culture bags would be the optimal approach with the gamma retroviral vector MSGV1-Hu19-CD828Z. The cell culture time for our Hu19-CAR T production process is 7 days. This compares favorably with total culture times for anti-CD19 CAR T cell production for recent CLL clinical trials, which ranged from 11 to 20 days.<sup>24–26</sup>

In summary, we rigorously explored T cell purification, T cell activation, and cytokine supplementation to optimize a clinical-scale GMP-compliant manufacturing protocol for producing Hu19-CAR T from CLL PBMC. The protocol incorporated CD4 plus CD8-positive selection, dyna activation, and media supplementation with IL-7+IL-15. With this protocol, Hu19-CAR T can be produced for use in clinical trials.

## MATERIALS AND METHODS

### Patient samples and mice

PBMCs were obtained from hematological malignancy patients enrolled on National Cancer Institute (NCI) clinical trials. Using patient samples for research was approved by the National Institutes of Health Institutional Review Board. Informed consent was obtained from all patients. Animal studies were approved by the NCI Animal Care and Use Committee.

### Cell lines

Cell lines used in the study were obtained from ATCC (Manassas, VA, USA). Toledo (B cell lymphoma), ST486 (Burkitt lymphoma), K562 (myeloid leukemia), and NALM6 (acute lymphoblastic leukemia). CCRF-CEM is a CD19-negative T cell leukemia cell line. CD19-K562 and NGFR-K562 are K562 cells transduced with the gene for full-length CD19 and the gene for low-affinity nerve growth factor, respectively, and were previously generated in our lab.<sup>64</sup> NALM6-GL were NALM6 cells stably transfected with green fluorescent protein and luciferase.

### T cell medium

T cells were cultured in T cell medium (TCM) in all experiments. TCM consisted of AIM V medium plus 5% AB serum (Gemini Bio Products, Woodland, CA, USA), 100 U/mL penicillin, and 100  $\mu$ g/mL streptomycin. All T cell cultures were supplemented with 10 ng/mL IL-7 + 5 ng/mL IL-15 (BRB Preclinical Repository NCI, Frederick, MD, USA) except for experiments reported in Figures 1 and S1 that utilized 300 IU/mL IL-2 (BRB Preclinical Repository NCI).

### CAR plasmids and vector

The Hu19 CAR was previously generated in our lab.<sup>36</sup> A codon-optimized DNA sequence of Hu19-CD828Z was designed and ligated into the MSGV1 gamma retroviral vector backbone. A producer cell clone for the MSGV1-Hu19-CD828Z vector was previously generated.<sup>65</sup> We also utilized the previously reported SP6-CD828Z negative-control CAR. SP6-CD828Z recognizes a small molecule

haptens but does not recognize human or mouse proteins.<sup>64</sup> GMP-compliant MSGV1-Hu19-CD828Z CAR vector used for experiments reported in [Figures 6](#) and [S6](#) was produced by the Indiana University Vector Production Facility.

#### Gamma-retroviral transduction and T cell culture

Human T cells were used in all experiments. Transduction of T cells with gamma-retroviruses was performed as previously described 2 days after initiation of T cell cultures.<sup>64</sup> T cells were cultured as described previously.<sup>64</sup> For the experiments described in [Figures 1](#) and [S1](#), PBMC were stimulated with the anti-CD3 monoclonal antibody OKT3 (Orthoclone, Bridgewater, NJ, USA). Non-tissue-culture-treated six-well plates were coated with Retronectin (Takara, Kusatsu, Japan). Two days after OKT3 stimulation, 2 mL gamma-retroviral vector supernatant was applied to each well of the retronectin-coated plates and incubated for 2 h at 37°C. Two milliliters of TCM containing  $2 \times 10^6$  cells were added directly to the vector supernatant. IL-2 or IL-7+IL-15 was added to the medium. Incubation was carried out at 37°C for 16–18 h. Next, cells were washed and suspended in fresh TCM with either IL-2 or IL-7+IL-15 added. Cultures were maintained by suspending the cells at  $0.5 \times 10^6$  cells/mL in TCM plus cytokines.

#### T cell purification in research-scale experiments

Patient PBMC were washed in TCM. PBMCs were then suspended in MACS buffer (containing 0.5% BSA, 2 mM EDTA in 1× PBS) and washed once. PBMC were then resuspended in MACS buffer at 80 µL per  $1 \times 10^7$  cells. The cells were then used in either the 19-dep or sel methods

#### CD19 depletion (19-dep)

The resuspended PBMC were labeled with human anti-CD19 Microbeads (Miltenyi Biotec, Gaithersburg, MD, USA) at a concentration of  $1 \times 10^7$  cells per 20 µL. The labeled cells were incubated for 15 min at 4°C, washed with MACS buffer once, and resuspended with MACS buffer at  $1 \times 10^8$  cells per 500 µL. The anti-CD19-Microbead-labeled cells were added to pre-rinsed LD Columns (Miltenyi Biotec, Bergisch Gladbach, Germany) and washed three times with MACS buffer. The supernatant flowing through the LD column was collected as the CD19-depleted fraction.

#### CD4 plus CD8 selection (sel)

Patient PBMCs were separately labeled with 20 µL of either human anti-CD4 or human anti-CD8 Microbeads (Miltenyi Biotec) per  $1 \times 10^7$  cells. The labeled cells were then incubated, washed, and resuspended with MACS buffer at a concentration of  $0.7 \times 10^8$  cells per 500 µL buffer. The anti-CD4 plus anti-CD8 microbead-labeled cells were individually added to pre-rinsed MS Columns (Miltenyi Biotec) and the columns were washed 3 times with 500 µL MACS buffer. The CD4<sup>+</sup> and CD8<sup>+</sup> T cells were bound to the MS columns. To elute T cells from the MS columns, columns were removed from the magnetic field and 1 mL MACS buffer was added. The cells were immediately flushed out by firmly pushing the plunger into the column. Eluted cells from CD4 plus CD8 selection were combined as enriched T cells.

#### Anti-CD3/CD28 dyna enrichment

Patient PBMCs were resuspended in isolation media (PBS without CaCl<sub>2</sub> and MgCl<sub>2</sub> with 1% human serum albumin) at a maximum of  $2 \times 10^8$  total cells per mL. Dynabeads<sup>TM</sup> (dyna) Human T-Expander anti-CD3/CD28 beads (Thermo Fisher Scientific, Rockville, MD, USA) were added to the PBMC suspension at a 3:1 ratio of beads to CD3<sup>+</sup> T cells, and the mixture was incubated for 30 min at room temperature. The dyna-bound cells were separated using a DYNAL MPC-1 Magnetic Particle Concentrator Separator (Dyna, Oslo, Norway). The dyna-bound cells were suspended in TCM supplemented with IL-7+IL-15 at  $1 \times 10^7$  cells/mL and cultured at 37°C.

#### T cell activation using immobilized anti-CD3/CD28 antibody in research-scale experiments

On day 0, T cells purified by the dep or sel methods were activated with one of three different formats of anti-CD3/anti-CD28: Dynabeads<sup>TM</sup> Human T-Expander CD3/CD28 (dyna) (Thermo Fisher Scientific), T cell Transact<sup>TM</sup> (trans) (Miltenyi Biotec), Cloudz human T cell activation kit (cloudz) (R&D system Inc., Minneapolis, MN, USA). Cloudz were dissolvable CD3/CD28 microspheres. For dyna activation, dyna were washed and added to the cell suspension ( $1 \times 10^6$  cells/mL) at a 3:1 bead:cell ratio. Dyna were removed on day 4 of cell culture using “The Big Easy” EasySep (Stemcell Technologies, Vancouver, Canada). For trans activation, T cells obtained from the 19-dep and sel methods were resuspended at  $2 \times 10^6$  cells/mL and  $1 \times 10^6$  cells/mL, respectively. Trans was added to the cell solution at a concentration of 10 µL/mL of cell suspension and was removed when media was changed as trans remained in the supernatant when cells were centrifuged. For cloudz activation, cells were resuspended at  $1 \times 10^6$  cells/mL. Fifty microliters and 20 µL of cloudz were added per 1 mL of cell suspension from the sel and 19-dep methods, respectively. On day 4 of cell culture, cloudz were removed by adding 6× release buffer in 6 mL cell solution. After T cell activation, gamma-retroviral transduction and T cell cultures were carried out as described under [“gamma-retroviral transduction and T cell culture.”](#) Transductions were initiated on day 2 of culture.

#### CAR detection and T cell phenotyping

Standard flow cytometry procedures were used as previously described.<sup>17</sup> Cell-surface CAR expression was detected with a non-commercial allophycocyanin (APC)-labeled antibody that binds the linker of the Hu19 scFv.<sup>17</sup> Antibodies were purchased from BD Biosciences (San Jose, CA, USA): CD3 APC-Cy7 (Clone UCHT1), CD4 brilliant violet 510 (Clone RPA-T4), CD8 R-phycoerythrin (PE)-Cy7/eFluor450 (Clone RPA-T8). The following antibodies were purchased from Biolegend: CD45RA fluorescein isothiocyanate (Clone HI100), CCR7 PE-Dazzle 594 (Clone G043H7), and CD95 PE (Clone DX2). Dead cells were excluded by using 7-amino-actinomycin D (7-AAD; BD Biosciences).

Flow cytometry was performed with a LSRFortessa (BD Biosciences) or FACSymphony A5 (BD Biosciences) cytometers. Flow cytometry analysis was performed using FlowJo (Tree Star, Inc., Ashland, OR, USA).

### CD107a assay

CD107a assays were performed as described previously.<sup>65</sup> Experimental tubes contained target cells, CAR-transduced T cells, 1 mL of TCM, PE-labeled anti-CD107a antibody (Clone H4A3, Thermo Fisher Scientific), and 1  $\mu$ L Golgi Stop (monensin, BD Biosciences). Tubes were incubated at 37°C for 4 h and then stained for CD3, CD4, and CD8. Samples were analyzed by flow cytometry. Normalization was conducted by dividing the percentage of CD4<sup>+</sup> or CD8<sup>+</sup> T cells that were CD107a<sup>+</sup> by the percentage of CD4<sup>+</sup> or CD8<sup>+</sup> T cells that were CAR<sup>+</sup>. Background degranulation with NGFR-K562 target cells was subtracted prior to data presentation.

### Cytotoxicity assay

Cytotoxicity assays were conducted as previously described.<sup>64–66</sup> Primary CLL patient PBMCs were thawed and cultured overnight in TCM and used as positive target cells for cytotoxicity. The cytotoxicity of Hu19-CAR T was measured by comparing survival of primary CLL target cells relative to the survival of negative-control, CD19-negative, CCRF-CEM cells. Both cell types were combined in the same tubes with CAR-transduced T cells. CCRF-CEM cells were labeled with 5-(and-6)-(((4-chloromethyl)benzoyl)amino) tetramethylrhodamine (Thermo Fisher Scientific), and CLL cells were labeled with CFSE (Thermo Fisher Scientific). Duplicate cultures were set up in sterile 5 mL test tubes (BD Bioscience) at multiple T cell to target cell ratios. Fifty thousand CLL cells and 50,000 CCRF-CEM cells were included in each tube. Cultures were incubated for 4 h at 37°C. Immediately after the incubation, 7-AAD was added, and flow cytometry acquisition was performed. For each T cell plus target cell culture, the percent survival of CLL cells was determined by dividing the percent live CLL cells by the percent live CCRF-CEM negative-control cells. The corrected percent survival of cells was calculated by dividing the percent survival of CLL cells in each T cell plus target cell culture by the ratio of the percent live CLL cells to the percent live CCRF-CEM cells in tubes containing only CLL cells and CCRF-CEM cells without effector T cells. This correction was necessary to account for variation in the starting cell numbers and for spontaneous target cell death. Cytotoxicity was calculated as follows: the percent cytotoxicity of CLL target cells = 100-corrected percent survival of CLL target cells.

### IFN- $\gamma$ and IL-2 ELISAs

CD19<sup>+</sup> or CD19-negative target cells were co-cultured with Hu19-CAR T at a 1:1 effector to target ratio at 37°C for 18–20 h. Following the incubation, IFN- $\gamma$  ELISAs were performed using standard methods (Pierce, Rockford, IL, USA). IL-2 ELISAs (R&D Systems, Minneapolis, MN, USA) were performed following the manufacturer's recommendations. T cells were washed and added to ELISA plates in medium that did not contain exogenous IL-2.

### Proliferation assays

Proliferation assays were set up as described previously.<sup>67,68</sup> In brief,  $0.5 \times 10^6$  irradiated CD19-K562 or irradiated NGFR-K562 cells were co-cultured with CFSE-labeled Hu19-CAR T for 4 days. After 4 days, the live cells in each co-culture were counted with tripan blue dead-

cell exclusion. Flow cytometry was performed for CFSE, CAR, CD3, CD4, and CD8. CD19-specific proliferation was presented as the CFSE median fluorescence intensity (MFI) of T cells stimulated with CD19-K562 divided by the CFSE MFI of T cells stimulated with NGFR-K562. Fold change from day 0 to day 4 was calculated by dividing the absolute number of CAR<sup>+</sup> T cells on day 4 with the absolute number of CAR<sup>+</sup> T cells on day 0.

### Murine solid tumor experiments

Solid tumor experiments were carried out as described previously.<sup>65</sup> Seven- to 9-week-old female NSG mice (NOD.Cg-Prkdc<sup>scid</sup> Il2rg<sup>tm1Wjl</sup>/SzJ) from the NCI-Frederick or the Jackson Laboratories (Bar Harbor, ME, USA) were used. We injected  $4 \times 10^6$  ST486 cells intradermally in a 1:1 mix of Matrigel (Corning, Corning, NY, USA) and PBS 6 days prior to CAR T cell injection. All mice in the experiment had measurable tumors prior to CAR T cell injection. CAR T cells from cultures initiated seven days prior to injection were injected intravenously at CD3<sup>+</sup>CAR<sup>+</sup> cell doses indicated in figure legends. Mice received one CAR T cell injection. Mice were sacrificed when the longest tumor length reached 15 mm. Tumors were measured with a caliper every three days, and the volume of the tumors was calculated using the formula (length  $\times$  width  $\times$  height)/2. Tumor volume curves ended when the first mouse of a group was sacrificed, or the experiment ended.

### Murine disseminated leukemia experiments

Seven- to 9-week-old, female NSG mice were intravenously injected with  $2 \times 10^6$  NALM6-GL cells. Three days later, mice were infused with Hu19-CAR T at the doses indicated in the figure legends. Mice received one CAR T cell infusion for all experiments. Bioluminescent images of mice were taken on the day of CAR T cell infusion and every 3 days thereafter. Imaging was done as follows: mice were intraperitoneally injected with 200  $\mu$ L of 15 mg/mL luciferin solution (GoldBio, Olivette, MO, USA). Bioluminescent images were taken 10 min after luciferin injection, while the mice were under anesthesia with 3% isoflurane. Images were captured using Xenogen IVIS Imaging System with Living Imaging software. Ventral images were captured at 30 s exposures on a 24-cm field of view and at binning factor of 4. Bioluminescence was quantified as the body of the mouse without the tail in units of radiance (p/sec/cm<sup>2</sup>/sr) using the Living Image software (Xenogen, Alameda, CA, USA). Mice were sacrificed in accordance with the NCI Animal Care and Use Committee guidelines.

### Rtx treatment in mouse experiments

Rtx (Genentech, San Francisco, CA, USA) and control IgG (Gamunex-C 10% from Grifols USA, Los Angeles, CA, USA) were purchased from NIH Veterinary Pharmacy (Bethesda, MD, USA). As described in figure legends for both solid tumor and disseminated tumor experiments, mice received intraperitoneal injections of 200  $\mu$ g of either Rtx or Ig 6 h before CAR T cell infusion. This dose was based on prior work by other investigators.<sup>69</sup> Antibody injections were then repeated at 200  $\mu$ g per dose every Monday, Wednesday, and Friday up to day 30 after CAR T cell infusion or until the mice reached the criteria for euthanasia.

### Clinical-scale CD4 and CD8 selection from PBMC

PBMC apheresis products were collected according to standard procedures. Apheresis cells were counted, and flow cytometry was performed to evaluate the frequencies of cells expressing CD3, CD4, CD8, and CD19 prior to CD4 plus CD8 T cell selection. For CD4 plus CD8 selection, apheresis products were labeled with anti-CD4 and anti-CD8 microbeads, and column purification was performed with a CliniMACS Plus device (Miltenyi Biotec).

### Clinical transduction and culture of T cells

T cell cultures were initiated using either freshly purified CD4 and CD8 T cells or cryopreserved CD4 and CD8 T cells. The cells were placed into Origen Permalife bags at a concentration of  $1 \times 10^6$  viable cells/mL in complete media (CM) containing Cell Therapy Systems (CTS) AIM V medium, 10 ng/mL IL-7 (Miltenyi Biotec), 5 ng/mL IL-15 (Miltenyi Biotec), 2 mM GlutaMax, and 5% human AB serum. T cells were then stimulated with CTS CD3/CD28 dyna (Thermo Fisher Scientific) at a 3:1 dyna to cells ratio. On day 2, T cells were transduced with GMP-compliant MSGV1-Hu19-CD828Z CAR vector at a cell concentration of  $0.5 \times 10^6$  viable cells/mL by first incubating vector in retronectin coated bags for 2 h and then adding cells in CM for a final vector dilution of 1 part vector plus 4 parts CM. After 22–24 h, vector+media was removed to stop transduction. On day 4, dyna were removed by using a CTS DynaMag Magnet (Thermo Fisher Scientific). The CAR T cell cultures were diluted to a concentration of  $0.5 \times 10^6$  viable cells/mL with CM on days 3, 4, and 5 of culture. The target date for harvest was day 7, with an extension to day 9 if necessary to achieve the clinical dose. For these test experiments, cultures were extended to day 9. Viable cells were enumerated during the culture on days 2, 3, 4, 5, 7, and 9. Safety studies were performed in accordance with the guidance from the U.S. Food and Drug Administration: current GMPs for phase I investigational drugs, and included testing for sterility, mycoplasma, endotoxin, vector copy number, and recombinant retrovirus.<sup>70</sup>

### Statistics

Statistics were performed with GraphPad Prism Version 8.4.3. A *p* value of less than 0.05 was considered statistically significant. Details of statistics and the number of replicates are provided in the figure legends.

### DATA AND CODE AVAILABILITY

Questions about data and requests for materials can be addressed to the corresponding author. Upon reasonable request we will provide materials not commercially available that were used in this work.

### SUPPLEMENTAL INFORMATION

Supplemental information can be found online at <https://doi.org/10.1016/j.omtm.2024.101212>.

### ACKNOWLEDGMENTS

This work was supported in part by the National Cancer Institute, National Institutes of Health intramural funding. This work was supported in part by a research agreement between Kite, a Gilead Com-

pany, and the NCI. We thank the animal care staff of the National Institutes of Health (NIH) Clinical Research Center animal facility. We also thank the staff of the National Cancer Institute (NCI), Surgery Branch flow cytometry core facility.

### AUTHOR CONTRIBUTIONS

C.A. planned experiments, conducted experiments, and wrote the manuscript; K.A.W., V.F., N.L., D.A.N., and L.C.C. conducted experiments; S.L.H. supervised and planned experiments; J.N.K. supervised experiments, planned experiments, and wrote the manuscript. All authors edited the manuscript.

### DECLARATION OF INTERESTS

J.K. and N.L. are inventors on patent applications for the Hu19-CD828Z CAR reported in this manuscript, and J.K. is Principal Investigator of a research agreement that involves NCI receiving research funding from Kite, a Gilead Company.

### REFERENCES

1. Cancer Stat Facts: Leukemia-Chronic Lymphocytic Leukemia (CLL). <https://seer.cancer.gov/statfacts/html/clyl.html>.
2. Bosch, F., and Dalla-Favera, R. (2019). Chronic lymphocytic leukaemia: from genetics to treatment. *Nat. Rev. Clin. Oncol.* 16, 684–701. <https://doi.org/10.1038/s41571-019-0239-8>.
3. Eichhorst, B., Robak, T., Montserrat, E., Ghia, P., Niemann, C.U., Kater, A.P., Gregor, M., Cymbalista, F., Buske, C., Hillmen, P., et al. (2021). Chronic lymphocytic leukaemia: ESMO Clinical Practice Guidelines for diagnosis, treatment and follow-up. *Ann. Oncol.* 32, 23–33. <https://doi.org/10.1016/j.annonc.2020.09.019>.
4. Patel, K., and Pagel, J.M. (2021). Current and future treatment strategies in chronic lymphocytic leukemia. *J. Hematol. Oncol.* 14, 69. <https://doi.org/10.1186/s13045-021-01054-w>.
5. James, D.F., and Kipps, T.J. (2011). Rituximab in chronic lymphocytic leukemia. *Adv. Ther.* 28, 534–554. <https://doi.org/10.1007/s12325-011-0032-2>.
6. Byrd, J.C., Murphy, T., Howard, R.S., Lucas, M.S., Goodrich, A., Park, K., Pearson, M., Waselenko, J.K., Ling, G., Grever, M.R., et al. (2001). Rituximab using a thrice weekly dosing schedule in B-cell chronic lymphocytic leukemia and small lymphocytic lymphoma demonstrates clinical activity and acceptable toxicity. *J. Clin. Oncol.* 19, 2153–2164. <https://doi.org/10.1200/JCO.2001.19.8.2153>.
7. Zhao, Z., Grégoire, C., Oliveira, B., Chung, K., and Melenhorst, J.J. (2023). Challenges and opportunities of CAR T-cell therapies for CLL. *Semin. Hematol.* 60, 25–33. <https://doi.org/10.1053/j.seminhematol.2023.01.002>.
8. Shadman, M., and Maloney, D.G. (2021). Immune Therapy for Chronic Lymphocytic Leukemia: Allogeneic Transplant, Chimeric Antigen Receptor T-cell Therapy, and Beyond. *Hematol. Oncol. Clin. N. Am.* 35, 847–862. <https://doi.org/10.1016/j.hoc.2021.03.011>.
9. Mikkilineni, L., and Kochenderfer, J.N. (2021). CAR T cell therapies for patients with multiple myeloma. *Nat. Rev. Clin. Oncol.* 18, 71–84. <https://doi.org/10.1038/s41571-020-0427-6>.
10. Cappell, K.M., and Kochenderfer, J.N. (2021). A comparison of chimeric antigen receptors containing CD28 versus 4-1BB costimulatory domains. *Nat. Rev. Clin. Oncol.* 18, 715–727. <https://doi.org/10.1038/s41571-021-00530-z>.
11. Milone, M.C., Xu, J., Chen, S.J., Collins, M.A., Zhou, J., Powell, D.J., Jr., and Melenhorst, J.J. (2021). Engineering-enhanced CAR T cells for improved cancer therapy. *Nat. Can. (Ott.)* 2, 780–793. <https://doi.org/10.1038/s43018-021-00241-5>.
12. Brudno, J.N., and Kochenderfer, J.N. (2018). Chimeric antigen receptor T-cell therapies for lymphoma. *Nat. Rev. Clin. Oncol.* 15, 31–46. <https://doi.org/10.1038/nrclinonc.2017.128>.
13. Abramson, J.S., Palomba, M.L., Gordon, L.I., Lunning, M.A., Wang, M., Arnason, J., Mehta, A., Purev, E., Maloney, D.G., Andreadis, C., et al. (2020). Lisocabtagene

- maraleucel for patients with relapsed or refractory large B-cell lymphomas (TRANSCEND NHL 001): a multicentre seamless design study. *Lancet* 396, 839–852. [https://doi.org/10.1016/S0140-6736\(20\)31366-0](https://doi.org/10.1016/S0140-6736(20)31366-0).
14. Locke, F.L., Ghobadi, A., Jacobson, C.A., Miklos, D.B., Lekakis, L.J., Oluwole, O.O., Lin, Y., Braunschweig, I., Hill, B.T., Timmerman, J.M., et al. (2019). Long-term safety and activity of axicabtagene ciloleucel in refractory large B-cell lymphoma (ZUMA-1): a single-arm, multicentre, phase 1–2 trial. *Lancet Oncol.* 20, 31–42. [https://doi.org/10.1016/S1470-2045\(18\)30864-7](https://doi.org/10.1016/S1470-2045(18)30864-7).
  15. Maude, S.L., Laetsch, T.W., Buechner, J., Rives, S., Boyer, M., Bittencourt, H., Bader, P., Verrieris, M.R., Stefanski, H.E., Myers, G.D., et al. (2018). Tisagenlecleucel in children and young adults with B-cell lymphoblastic leukemia. *N. Engl. J. Med.* 378, 439–448. <https://doi.org/10.1056/NEJMoa1709866>.
  16. Lee, D.W., Kochenderfer, J.N., Stetler-Stevenson, M., Cui, Y.K., Delbrook, C., Feldman, S.A., Fry, T.J., Orentas, R., Sabatino, M., Shah, N.N., et al. (2015). T cells expressing CD19 chimeric antigen receptors for acute lymphoblastic leukaemia in children and young adults: A phase 1 dose-escalation trial. *Lancet* 385, 517–528. [https://doi.org/10.1016/S0140-6736\(14\)61403-3](https://doi.org/10.1016/S0140-6736(14)61403-3).
  17. Brudno, J.N., Lam, N., Vanasse, D., Shen, Y.W., Rose, J.J., Rossi, J., Xue, A., Bot, A., Scholler, N., Mikkilineni, L., et al. (2020). Safety and feasibility of anti-CD19 CAR T cells with fully human binding domains in patients with B-cell lymphoma. *Nat. Med.* 26, 270–280. <https://doi.org/10.1038/s41591-019-0737-3>.
  18. Cappell, K.M., Sherry, R.M., Yang, J.C., Goff, S.L., Vanasse, D.A., McIntyre, L., Rosenberg, S.A., and Kochenderfer, J.N. (2020). Long-Term Follow-Up of Anti-CD19 Chimeric Antigen Receptor T-Cell Therapy. *J. Clin. Oncol.* 38, 3805–3815. <https://doi.org/10.1200/JCO.20.01467>.
  19. Matutes, E., and Polliack, A. (2000). Morphological and immunophenotypic features of chronic lymphocytic leukemia. *Rev. Clin. Exp. Hematol.* 4, 22–47. <https://doi.org/10.1046/j.1468-0734.2000.00002.x>.
  20. Kochenderfer, J.N., Dudley, M.E., Kassim, S.H., Somerville, R.P.T., Carpenter, R.O., Stetler-Stevenson, M., Yang, J.C., Phan, G.Q., Hughes, M.S., Sherry, R.M., et al. (2015). Chemotherapy-refractory diffuse large B-cell lymphoma and indolent B-cell malignancies can be effectively treated with autologous T cells expressing an anti-CD19 chimeric antigen receptor. *J. Clin. Oncol.* 33, 540–549. <https://doi.org/10.1200/JCO.2014.56.2025>.
  21. Brentjens, R.J., Riviere, I., Park, J.H., Davila, M.L., Wang, X., Stefanski, J., Taylor, C., Yeh, R., Bartido, S., Borquez-Ojeda, O., et al. (2011). Safety and persistence of adoptively transferred autologous CD19-targeted T cells in patients with relapsed or chemotherapy refractory B-cell leukemias. *Blood* 118, 4817–4828.
  22. Kalos, M., Levine, B.L., Porter, D.L., Katz, S., Grupp, S.A., Bagg, A., and June, C.H. (2011). T cells with chimeric antigen receptors have potent antitumor effects and can establish memory in patients with advanced leukemia. *Sci. Transl. Med.* 3, 95ra73.
  23. Kochenderfer, J.N., Dudley, M.E., Feldman, S.A., Wilson, W.H., Spaner, D.E., Maric, I., Stetler-Stevenson, M., Phan, G.Q., Hughes, M.S., Sherry, R.M., et al. (2012). B-cell depletion and remissions of malignancy along with cytokine-associated toxicity in a clinical trial of anti-CD19 chimeric-antigen-receptor-transduced T cells. *Blood* 119, 2709–2720.
  24. Turtle, C.J., Hay, K.A., Hanafi, L.A., Li, D., Cherian, S., Chen, X., Wood, B., Lozanski, A., Byrd, J.C., Heimfeld, S., et al. (2017). Durable molecular remissions in chronic lymphocytic leukemia treated with CD19-specific chimeric antigen Receptor-modified T cells after failure of ibrutinib. *J. Clin. Oncol.* 35, 3010–3020. <https://doi.org/10.1200/JCO.2017.72.8519>.
  25. Porter, D.L., Hwang, W.T., Frey, N.V., Lacey, S.F., Shaw, P.A., Loren, A.W., Bagg, A., Marcucci, K.T., Shen, A., Gonzalez, V., et al. (2015). Chimeric antigen receptor T cells persist and induce sustained remissions in relapsed refractory chronic lymphocytic leukemia. *Sci. Transl. Med.* 7, 303ra139. <https://doi.org/10.1126/scitranslmed.aac5415>.
  26. Frey, N.V., Gill, S., Hexner, E.O., Schuster, S., Nasta, S., Loren, A., Svoboda, J., Stadtmauer, E., Landsburg, D.J., Mato, A., et al. (2020). Long-Term Outcomes From a Randomized Dose Optimization Study of Chimeric Antigen Receptor Modified T Cells in Relapsed Chronic Lymphocytic Leukemia. *J. Clin. Oncol.* 38, 2862–2871. <https://doi.org/10.1200/jco.19.03237>.
  27. Siddiqi, T., Maloney, D.G., Kenderian, S.S., Brander, D.M., Dorritie, K., Soumerai, J., Riedell, P.A., Shah, N.N., Nath, R., Fakhri, B., et al. (2023). Lisocabtagene maraleucel in chronic lymphocytic leukaemia and small lymphocytic lymphoma (TRANSCEND CLL 004): a multicentre, open-label, single-arm, phase 1–2 study. *Lancet* 402, 641–654. [https://doi.org/10.1016/S0140-6736\(23\)01052-8](https://doi.org/10.1016/S0140-6736(23)01052-8).
  28. Schuster, S.J., Bishop, M.R., Tam, C.S., Waller, E.K., Borchmann, P., McGuirk, J.P., Jäger, U., Jaglowski, S., Andreadis, C., Westin, J.R., et al. (2019). Tisagenlecleucel in adult relapsed or refractory diffuse large B-cell lymphoma. *N. Engl. J. Med.* 380, 45–56. <https://doi.org/10.1056/NEJMoa1804980>.
  29. Hallek, M., Cheson, B.D., Catovsky, D., Caligaris-Cappio, F., Dighiero, G., Döhner, H., Hillmen, P., Keating, M., Montserrat, E., Chiorazzi, N., et al. (2018). iwCLL guidelines for diagnosis, indications for treatment, response assessment, and supportive management of CLL. *Blood* 131, 2745–2760. <https://doi.org/10.1182/blood-2017-09-806398>.
  30. Riches, J.C., Davies, J.K., McClanahan, F., Fatah, R., Iqbal, S., Agrawal, S., Ramsay, A.G., and Gribben, J.G. (2013). T cells from CLL patients exhibit features of T-cell exhaustion but retain capacity for cytokine production. *Blood* 121, 1612–1621. <https://doi.org/10.1182/blood-2012-09-457531>.
  31. Ramsay, A.G., Johnson, A.J., Lee, A.M., Gorgün, G., Le Dieu, R., Blum, W., Byrd, J.C., and Gribben, J.G. (2008). Chronic lymphocytic leukemia T cells show impaired immunological synapse formation that can be reversed with an immunomodulating drug. *J. Clin. Invest.* 118, 2427–2437. <https://doi.org/10.1172/JCI35017>.
  32. Fraietta, J.A., Lacey, S.F., Orlando, E.J., Pruteanu-Malinici, I., Gohil, M., Lundh, S., Boesteanu, A.C., Wang, Y., O'Connor, R.S., Hwang, W.T., et al. (2018). Determinants of response and resistance to CD19 chimeric antigen receptor (CAR) T cell therapy of chronic lymphocytic leukemia. *Nat. Med.* 24, 563–571. <https://doi.org/10.1038/s41591-018-0010-1>.
  33. Turtle, C.J., Hay, K.A., Hanafi, L.A., Li, D., Cherian, S., Chen, X., Wood, B., Lozanski, A., Byrd, J.C., Heimfeld, S., et al. (2017). Durable Molecular Remissions in Chronic Lymphocytic Leukemia Treated With CD19-Specific Chimeric Antigen Receptor-Modified T Cells After Failure of Ibrutinib. *J. Clin. Oncol.* 35, 3010–3020. <https://doi.org/10.1200/JCO.2017.72.8519>.
  34. Xu, Y., Zhang, M., Ramos, C.A., Durett, A., Liu, E., Dakhova, O., Liu, H., Creighton, C.J., Gee, A.P., Heslop, H.E., et al. (2014). Closely related T-memory stem cells correlate with in vivo expansion of CAR-CD19-T cells and are preserved by IL-7 and IL-15. *Blood* 123, 3750–3759. <https://doi.org/10.1182/blood-2014-01-552174>.
  35. Zhou, J., Jin, L., Wang, F., Zhang, Y., Liu, B., and Zhao, T. (2019). Chimeric antigen receptor T (CAR-T) cells expanded with IL-7/IL-15 mediate superior antitumor effects. *Protein Cell* 10, 764–769. <https://doi.org/10.1007/s13238-019-0643-y>.
  36. Alabanza, L., Pegues, M., Geldres, C., Shi, V., Wiltzius, J.J.W., Sievers, S.A., Yang, S., and Kochenderfer, J.N. (2017). Function of Novel Anti-CD19 Chimeric Antigen Receptors with Human Variable Regions Is Affected by Hinge and Transmembrane Domains. *Mol. Ther.* 25, 2452–2465. <https://doi.org/10.1016/j.ymthe.2017.07.013>.
  37. Seitter, S.J., McClelland, P.H., Ahlman, M.A., Goff, S.L., Yang, J.C., McIntyre, L., Rosenberg, S.A., Kochenderfer, J.N., and Brudno, J.N. (2022). Durable remissions in two adult patients with Burkitt lymphoma following anti-CD19 CAR T-cell therapy: a single center experience. *Leuk. Lymphoma* 63, 2469–2473. <https://doi.org/10.1080/10428194.2022.2076853>.
  38. Hughes, M.S., Yu, Y.Y.L., Dudley, M.E., Zheng, Z., Robbins, P.F., Li, Y., Wunderlich, J., Hawley, R.G., Moayeri, M., Rosenberg, S.A., and Morgan, R.A. (2005). Transfer of a TCR gene derived from a patient with a marked antitumor response conveys highly active T-cell effector functions. *Hum. Gene Ther.* 16, 457–472.
  39. Muroyama, Y., and Wherry, E.J. (2021). Memory t-cell heterogeneity and terminology. *Cold Spring Harbor Perspect. Biol.* 13, a037929. <https://doi.org/10.1101/cshperspect.a037929>.
  40. Sallusto, F., Lenig, D., Förster, R., Lipp, M., and Lanzavecchia, A. (1999). Two subsets of memory T lymphocytes with distinct homing potentials and effector functions. *Nature* 401, 708–712.
  41. Brown, C.E., Alizadeh, D., Starr, R., Weng, L., Wagner, J.R., Naranjo, A., Ostberg, J.R., Blanchard, M.S., Kilpatrick, J., Simpson, J., et al. (2016). Regression of Glioblastoma after Chimeric Antigen Receptor T-Cell Therapy. *N. Engl. J. Med.* 375, 2561–2569. <https://doi.org/10.1056/NEJMoa1610497>.
  42. Brentjens, R.J., Davila, M.L., Riviere, I., Park, J., Wang, X., Cowell, L.G., Bartido, S., Stefanski, J., Taylor, C., Olszewska, M., et al. (2013). CD19-targeted T cells rapidly induce molecular remissions in adults with chemotherapy-refractory acute

- lymphoblastic leukemia. *Sci. Transl. Med.* 5, 177ra38–177ra138. <https://doi.org/10.1126/scitranslmed.3005930>.
43. Tumaini, B., Lee, D.W., Lin, T., Castiello, L., Stroncek, D.F., Mackall, C., Wayne, A., and Sabatino, M. (2013). Simplified process for the production of anti-CD19-CAR-engineered T cells. *Cytotherapy* 15, 1406–1415. <https://doi.org/10.1016/j.jcyt.2013.06.003>.
  44. Cordoba, S., Onuoha, S., Thomas, S., Pignataro, D.S., Hough, R., Ghorashian, S., Vora, A., Bonney, D., Veys, P., Rao, K., et al. (2021). CAR T cells with dual targeting of CD19 and CD22 in pediatric and young adult patients with relapsed or refractory B cell acute lymphoblastic leukemia: a phase 1 trial. *Nat. Med.* 27, 1797–1805. <https://doi.org/10.1038/s41591-021-01497-1>.
  45. (2023). <https://www.miltenybiotec.com/US-en/applications/all-protocols/engineering-of-car-t-cells-for-research-use.html>.
  46. (2020). Cloudz Human T Cell Activation Kit. [https://www.rndsystems.com/products/cloudz-human-t-cell-activation-kit\\_cld001#product-datashets](https://www.rndsystems.com/products/cloudz-human-t-cell-activation-kit_cld001#product-datashets).
  47. Ramsay, A.G., Clear, A.J., Fatah, R., and Gribben, J.G. (2012). Multiple inhibitory ligands induce impaired T-cell immunologic synapse function in chronic lymphocytic leukemia that can be blocked with lenalidomide: Establishing a reversible immune evasion mechanism in human cancer. *Blood* 120, 1412–1421. <https://doi.org/10.1182/blood-2012-02-411678>.
  48. Magalhaes, I., Kalland, I., Kochenderfer, J.N., Österborg, A., Uhlin, M., and Mattsson, J. (2018). CD19 Chimeric Antigen Receptor T Cells from Patients with Chronic Lymphocytic Leukemia Display an Elevated IFN- $\gamma$  Production Profile. *J. Immunother.* 41, 73–83. <https://doi.org/10.1097/CJI.0000000000000193>.
  49. Gargett, T., Yu, W., Dotti, G., Yvon, E.S., Christo, S.N., Hayball, J.D., Lewis, I.D., Brenner, M.K., and Brown, M.P. (2016). GD2-specific CAR T Cells Undergo Potent Activation and Deletion Following Antigen Encounter but can be Protected from Activation-induced Cell Death by PD-1 Blockade. *Mol. Ther.* 24, 1135–1149. <https://doi.org/10.1038/mt.2016.63>.
  50. Lesch, S., Benmebarek, M.R., Cadilha, B.L., Stoiber, S., Subklewe, M., Endres, S., and Kobold, S. (2020). Determinants of response and resistance to CAR T cell therapy. *Semin. Cancer Biol.* 65, 80–90. <https://doi.org/10.1016/j.semcancer.2019.11.004>.
  51. Noaks, E., Peticone, C., Kotsopoulou, E., and Bracewell, D.G. (2021). Enriching leukapheresis improves T cell activation and transduction efficiency during CAR T processing. *Mol. Ther. Methods Clin. Dev.* 20, 675–687. <https://doi.org/10.1016/j.omtm.2021.02.002>.
  52. Arcangeli, S., Falcone, L., Camisa, B., De Girardi, F., Biondi, M., Giglio, F., Ciceri, F., Bonini, C., Bondanza, A., and Casucci, M. (2020). Next-Generation Manufacturing Protocols Enriching T(SCM) CAR T Cells Can Overcome Disease-Specific T Cell Defects in Cancer Patients. *Front. Immunol.* 11, 1217. <https://doi.org/10.3389/fimmu.2020.01217>.
  53. Kochenderfer, J.N., Somerville, R.P.T., Lu, T., Shi, V., Bot, A., Rossi, J., Xue, A., Goff, S.L., Yang, J.C., Sherry, R.M., et al. (2017). Lymphoma Remissions Caused by Anti-CD19 Chimeric Antigen Receptor T Cells Are Associated With High Serum Interleukin-15 Levels. *J. Clin. Oncol.* 35, 1803–1813. <https://doi.org/10.1200/jco.2016.71.3024>.
  54. Brudno, J.N., Maric, I., Hartman, S.D., Rose, J.J., Wang, M., Lam, N., Stetler-Stevenson, M., Salem, D., Yuan, C., Pavletic, S., et al. (2018). T cells genetically modified to express an anti-B-Cell maturation antigen chimeric antigen receptor cause remissions of poor-prognosis relapsed multiple myeloma. *J. Clin. Oncol.* 36, 2267–2280. <https://doi.org/10.1200/JCO.2018.77.8084>.
  55. Lin, Y., Rajee, N.S., Berdeja, J.G., Siegel, D.S., Jagannath, S., Madduri, D., Liedtke, M., Rosenblatt, J., Maus, M.V., Massaro, M., et al. (2023). Idecabtagene vicleucel for relapsed and refractory multiple myeloma: post hoc 18-month follow-up of a phase 1 trial. *Nat. Med.* 29, 2286–2294. <https://doi.org/10.1038/s41591-023-02496-0>.
  56. Gattinoni, L., Powell, D.J., Jr., Rosenberg, S.A., and Restifo, N.P. (2006). Adoptive immunotherapy for cancer: Building on success. *Nat. Rev. Immunol.* 6, 383–393. <https://doi.org/10.1038/nri1842>.
  57. Gattinoni, L., Klebanoff, C.A., Palmer, D.C., Wrzesinski, C., Kerstann, K., Yu, Z., Finkelstein, S.E., Theoret, M.R., Rosenberg, S.A., and Restifo, N.P. (2005). Acquisition of full effector function in vitro paradoxically impairs the in vivo antitumor efficacy of adoptively transferred CD8+ T cells. *J. Clin. Invest.* 115, 1616–1626. <https://doi.org/10.1172/JCI24480>.
  58. Ren, H., Cao, K., and Wang, M. (2021). A Correlation Between Differentiation Phenotypes of Infused T Cells and Anti-Cancer Immunotherapy. *Front. Immunol.* 12, 745109. <https://doi.org/10.3389/fimmu.2021.745109>.
  59. Deng, Q., Han, G., Puebla-Osorio, N., Ma, M.C.J., Strati, P., Chasen, B., Dai, E., Dang, M., Jain, N., Yang, H., et al. (2020). Characteristics of anti-CD19 CAR T cell infusion products associated with efficacy and toxicity in patients with large B cell lymphomas. *Nat. Med.* 26, 1878–1887. <https://doi.org/10.1038/s41591-020-1061-7>.
  60. Brudno, J.N., and Kochenderfer, J.N. (2019). Recent advances in CAR T-cell toxicity: Mechanisms, manifestations and management. *Blood Rev.* 34, 45–55. <https://doi.org/10.1016/j.blre.2018.11.002>.
  61. Mihara, K., Yanagihara, K., Takigahira, M., Kitanaka, A., Imai, C., Bhattacharyya, J., Kubo, T., Takei, Y., Yasunaga, S., Takihara, Y., and Kimura, A. (2010). Synergistic and persistent effect of T-cell immunotherapy with anti-CD19 or anti-CD38 chimeric receptor in conjunction with rituximab on B-cell non-Hodgkin lymphoma. *Br. J. Haematol.* 151, 37–46. <https://doi.org/10.1111/j.1365-2141.2010.08297.x>.
  62. James, S.E., Orgun, N.N., Tedder, T.F., Shlomchik, M.J., Jensen, M.C., Lin, Y., Greenberg, P.D., and Press, O.W. (2009). Antibody-mediated B-cell depletion before adoptive immunotherapy with T cells expressing CD20-specific chimeric T-cell receptors facilitates eradication of leukemia in immunocompetent mice. *Blood* 114, 5454–5463. <https://doi.org/10.1182/blood-2009-08-232967>.
  63. Brudno, J.N., and Kochenderfer, J.N. (2016). Toxicities of chimeric antigen receptor T cells: recognition and management. *Blood* 127, 3321–3330.
  64. Kochenderfer, J.N., Feldman, S.A., Zhao, Y., Xu, H., Black, M.A., Morgan, R.A., Wilson, W.H., and Rosenberg, S.A. (2009). Construction and preclinical evaluation of an anti-CD19 chimeric antigen receptor. *J. Immunother.* 32, 689–702.
  65. Lam, N., Finney, R., Yang, S., Choi, S., Wu, X., Cutmore, L., Andrade, J., Huang, L., Amaty, C., Cam, M., and Kochenderfer, J.N. (2023). Development of a bicistronic anti-CD19/CD20 CAR construct including abrogation of unexpected nucleic acid sequence deletions. *Mol. Ther. Oncolytics* 30, 132–149. <https://doi.org/10.1016/j.omto.2023.07.001>.
  66. Hermans, I.F., Silk, J.D., Yang, J., Palmowski, M.J., Gileadi, U., McCarthy, C., Salio, M., Ronchese, F., and Cerundolo, V. (2004). The VITAL assay: a versatile fluorometric technique for assessing CTL- and NKT-mediated cytotoxicity against multiple targets in vitro and in vivo. *J. Immunol. Methods* 285, 25–40. <https://doi.org/10.1016/j.jim.2003.10.017>.
  67. Amaty, C., Pegues, M.A., Lam, N., Vanasse, D., Geldres, C., Choi, S., Hewitt, S.M., Feldman, S.A., and Kochenderfer, J.N. (2021). Development of CAR T Cells Expressing a Suicide Gene Plus a Chimeric Antigen Receptor Targeting Signaling Lymphocytic-Activation Molecule F7. *Mol. Ther.* 29, 702–717. <https://doi.org/10.1016/j.ymthe.2020.10.008>.
  68. Lam, N., Trinklein, N.D., Buelow, B., Patterson, G.H., Ojha, N., and Kochenderfer, J.N. (2020). Author Correction: Anti-BCMA chimeric antigen receptors with fully human heavy-chain-only antigen recognition domains. *Nat. Commun.* 11, 1319. <https://doi.org/10.1038/s41467-020-15145-8>.
  69. Chao, M.P., Alizadeh, A.A., Tang, C., Myklebust, J.H., Varghese, B., Gill, S., Jan, M., Cha, A.C., Chan, C.K., Tan, B.T., et al. (2010). Anti-CD47 Antibody Synergizes with Rituximab to Promote Phagocytosis and Eradicate Non-Hodgkin Lymphoma. *Cell* 142, 699–713. <https://doi.org/10.1016/j.cell.2010.07.044>.
  70. U.S. Food and Drug Administration Center for Drug Evaluation and Research (2008). Guidance for Industry: cGMP for Phase 1 Investigational Drugs. <https://www.fda.gov/regulatory-information/search-fda-guidance-documents/current-good-manufacturing-practice-phase-1-investigational-drugs>.